Institut für Wissenschaftliches Rechnen

Prof. Hermann G. Matthies, Ph.D.

der TU Braunschweig

Jahresbericht 2013

Institut für Wissenschaftliches Rechnen der TU Braunschweig

Institutsvorstand:	Prof. Hermann G. Matthies, Ph.D.
Geschäftszimmer:	Frau Cosima Meyer, M.A.
Anschrift:	Institut für Wissenschaftliches Rechnen TU Braunschweig Hans-Sommer-Str. 65 38106 Braunschweig
Telefon, Telefax:	0531/391–3000, 0531/391–3003
E-Mail:	wire@tu-bs.de
URL:	http://www.wire.tu-bs.de

Wissenschaftliche Mitarbeiterinnen, Mitarbeiter und Doktoranden:

Frau Dr.-Ing. Noémi Friedman
Herr Dr. rer. nat. Thorsten Grahs
Herr Dr. rer. nat. Martin Krosche
Herr Dr. rer. nat. Alexander Litvinenko
Herr Dr.-Ing. Rainer Niekamp
Herr Dr. rer. nat. Joachim Rang
Frau Dr.-Ing. Bojana Rosić
Herr Dr. rer. nat. Elmar Zander

Assoziiert an der Tschechischen Technischen Universität Prag:

Frau Dr.-Ing. Anna Kučerová
Herr Dr.-Ing. Jan Sýkora

Apl. Professor: Herr Dr.-Ing. habil. Joachim Axmann (Volkswagen AG)

Centre for Scientific Computing:

Herr Dr. rer. nat. Thorsten Grahs

Externe Promovenden über das Deutsch-Italienische Promotionsprogramm: (alle DICeA - University of Florence)

Frau Ing. Valentina Chiarello
Herr Ing. Alberto Ciavattone
Herr Ing. Giovanni Stabile

Inhaltsverzeichnis

1 Vorwort

Dear Reader,

as the last year witnessed the completion of one habilitation and four doctoral theses, in 2013 there were no new ones, and we only have to report that these doctoral theses have now been published.

Looking at the research projects in 2013, some deal with coupled problems and software middleware for such computations, some with time integration methods, but most have in some way risk, stochastic, or identification as their topic. Stochastic Computations, or, as it is frequently called, „Uncertainty Quantification (UQ)“, is the underpinning for both considerations or risk measures as well as Bayesian identification. This seems to be a very exciting new area for modern low-rank approximations of stochastic variables, as it makes realistic computations feasible. I hope you, the reader, enjoy to see this interplay in the different projects at various stages.

Sincerely Yours

Hermann G. Matthies

2 Forschung

2.1 Stochastic Analysis of an Exotic Deployable Space Truss System

Ansprechpartner:	Noémi Friedman
EMail:	n.friedman@tu-bs.de
Telefon:	0531/391-3013

2.1.1 Introduction

Advanced deployable structures have appeared mainly for spatial engineering applications like booms, solar arrays, antennas, reflectors [6]. However, current trends try to apply these fascinating transformable systems in the field of civil engineering and architecture, like in off-shore industry and in provisory or dynamic architecture [4][1][3]. Nevertheless the related highly non-linear analysis can be very challenging even in the case of a simple system. Transformability usually costs; these structures are often very sensitive to small changes of physical parameters resulting in ill-posed problems when trying to model their behaviour.
Herein the investigation of a rather exotic type of cylindrical deployable structure is outlined. The original model of the analysed antiprismatic pop-up mast first offered by Hegedűs is derived from the Yoshimura-pattern and is rendered packable by stretchable hoop strut circles. Through the non-linear simulation it was found that by axially pushing the structure, the packing pattern of the mast depends on the material and geometric perturbations [2]. Deviating from the original model by replacing the alternately stiffened strut circles to elastic ones a new type of pop-up structure is formed that can be packed to a plane by expansion [1]. The packing patterns of this new system show a quite interesting chaotic system. However, the non-linear analysis of the structure has revealed that this pattern is chaotic though, but not completely stochastic. In fact, the possible deployment patterns - corresponding to the different parametric/geometric settings - are governed by difficultly determinable rules, resulting in regularities of the patterns resembling the fractal shapes derived from the Mandelbrot set.

2.1.2 Structural overview

The cylindrical deployable pop-up mast, first offered by Hegedűs [5], is rendered packable by stretchable hoop strut circles. Its basic unit formed by a truss system with bars placed on the edges of two regular superposed antiprisms (Figure 1a). The basic unit can be theoretically packed to a plain (if the dimension of the structure is not taken into

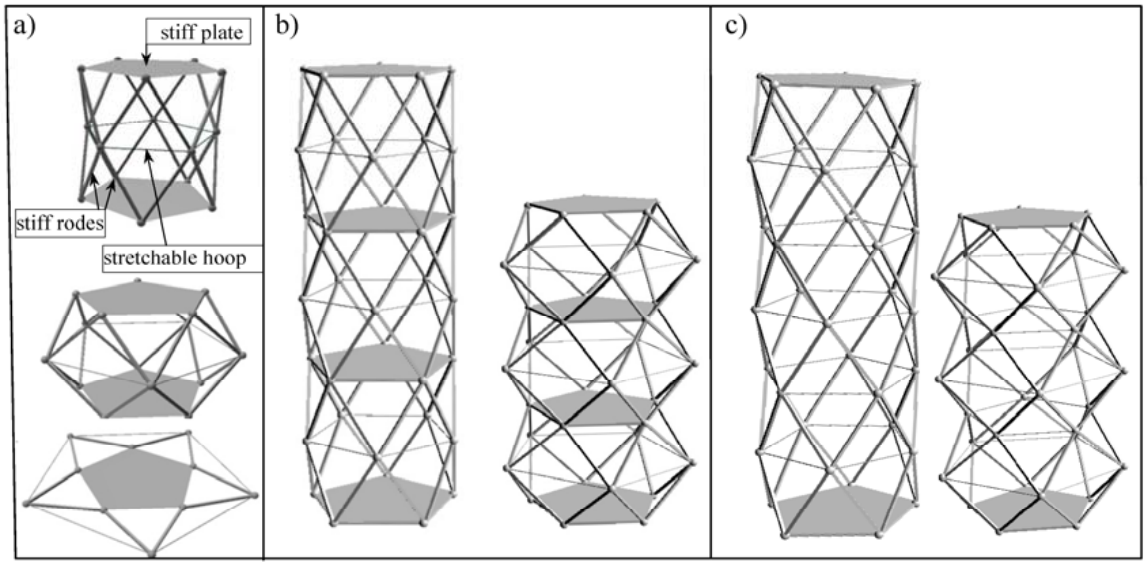

Figure 1: Basic unit (a), original pop-up mast(b), mast without inner stiffening(c)

account) by stretching the elastic bars of the inner polygon. By superposing this basic unit, a deployable mast is formed (Figure 1c). It was shown in [2], that by axially pushing the structure, the packing pattern of the mast is governed by the material and geometric perturbations, due to the branching of its equilibrium path.
By replacing the stiff plates by stretchable hoops, a new type of highly deformable pop-up structure is formed (Figure 1c) [1]. The packing pattern of this novel type of cylindrical truss system is much more complex.

2.1.3 Analysis

The packing of the antiprismatic mast was simulated with non-linear finite element analysis calculated with FEAP v 7.4. The analysis was carried out by controlling the displacement of the top nodes of the mast, while the bottom nodes were constrained. In the model, intersection of the struts was avoided by involving contact elements in between the segments. To trace the different packing paths, a self-developed simulation was run in MAPLE, based on an energetic approach. In this analysis the bifurcation paths were captured by a continuous, in-built random perturbation of the actual state of the system.
The non-linear simulations have shown that the packing pattern of the novel type of antiprismatic mast differs from the one of the original system. The mast of odd number of segments can be packed by expanding all its stretchable hoop strut circles. This packing is only possible if certain geometric packability conditions are satisfied. The mast of even number of segments first starts to expand its elastic polygonal elements, but afterwards begins to behave similarly to the original system. The elastic polygons start to alternately expand or contract. However, in contrast to the original system, the order of the closure of the segments

is not fully governed by the small perturbations. The analysis has proved that the pattern in not completely of stochastic nature but has regularities following some geometrical-mechanical rules.

References

[1] N. Friedman, *Investigation of highly flexible, deployable structures: Review, identification, control, application*, Ph.D. thesis, ENS de Cachan and Budapest University of Technology and Economics, 2011, URL: hal.archives-ouvertes.fr/docs/00/67/54/81/PDF/Friedman2011.pdf.

[2] N. Friedman, M. Weiner, Gy. Farkas, I. Hegedűs, and A. Ibrahimbegović, *On the snap-back behavior of a self-deploying antiprismatic column during packing*, Engineering Structures **50** (2013), 74–89, doi:10.1016/j.engstruct.2012.12.035.

[3] N. Friedman and Gy. Farkas, *Roof structures in motion - on retractable and deployable roof structures enabling quick construction or adaption to external excitations*, Concrete Structures (2011), 41–50, URL: http://fib.bme.hu/cs2011/CS_2011.html.

[4] C. J. Gantes, *Deployable structures: analysis and design*, Wit Press, 2001.

[5] I. Hegedűs, *Branching of equilibrium paths in a deployable column*, International Journal of Space Structures **8** (1993), 119–125.

[6] S. Pellegrino, *Deployable structures*, CISM International Centre for Mechanical Sciences, Springer, 2001.

2.2 Non-intrusive stochastic Galerkin method for uncertainty quantification of ordinary differential equations

Ansprechpartner:	Noémi Friedman
EMail:	n.friedman@tu-bs.de
Telefon:	0531/391-3013

2.2.1 Introduction

The dynamically growing field of uncertainty quantification is just starting to enter into engineering practice. However, the most popular methods among engineers still remain the brute force Monte Carlo type of sampling based methods [2] [9], mainly because of their simplicity. These methods necessitate an excessive computational burden, as for accurate statistical information a large number of executions of the deterministic simulation is needed. However, its simplicity and decoupled, non-intrusive manner to calculate the impact of uncertainties still seem to keep these methods an attractive choice. In the case of a complex model, or in the case of commercial software without the possibility to change the solver, one indeed needs a non-intrusive method to quantify uncertainties of the model.
Engineers are less familiar with other non-intrusive methods enabling the use of the original solver, using proxy models, like collocation methods [1], or discrete projections [3] [8], but with a significantly release of the computational burden. However these methods have the disadvantage that the proxy model may not satisfy everywhere the parametric equation. That is one of the reasons why the coupled, Galerkin-type methods [5] [7], incorporating the uncertainties in the solver itself have become one of the most widely celebrated methods among scientist. The main problem with the Galerkin-type of methods is that it is not obvious how to apply the original solver.
Recently, it was shown in [6] how the coupled Galerkin method may be computed in a non-intrusive manner, avoiding the great amount of investment in building a new, stochastic solver, while ensuring the approximation to satisfy the parametric equation.
Herein a short outline of the investigation of applying this method to stochastic ODEs with explicit solvers is shown, with the goal of applying it in the future for the non-intrusive stochastic analysis of a nonlinear dynamic simulation model of a high-lift aircraft design (see Chapter 2.4.2 for further details). After the rough description of the algorithm in Section 2.2.2, some elementary numerical examples are presented in Section 2.2.3.

2.2.2 Non-intrusive stochastic Galerkin explicit time-integration

Let us suppose that we have a stochastic ODE in the form:

$$\dot{x}(t,\omega) = f(t, x(t,\omega), q(\omega)),$$

that we have to solve, where the variable x describes the state of the system, and the parameters q both depend on possible realisations $\omega \in \Omega$ (where Ω is the probability space), that is both are random variables. Suppose also that we have an explicit integrator, convergent for all values of q, that simulates our physical system by generating the solution for successive time steps:

$$x_{k+1} = x_k + \Delta x_k = x_k(q) + S\left(\Delta t, q, x_k(q)\right)$$

where S is one cycle of the numerical time-stepping integrator.

By substituting a proxy model of x_k and x_{k+1}, for example by approximating them with a gPCE [11] using orthogonal polynomials:

$$x_k \cong \sum_\alpha x_k^{(\alpha)} \psi_\alpha\left(\theta(\omega)\right)$$

$$x_{k+1} \cong \sum_\alpha x_{k+1}^{(\alpha)} \psi_\alpha\left(\theta(\omega)\right)$$

where $\psi_\alpha\left(\theta(\omega)\right)$ are the orthogonal polynomials and $\theta(\omega)$ are some known random variables, the time-stepping becomes:

$$\sum_\alpha x_{k+1}^{(\alpha)} \psi_\alpha\left(\theta\right) = \sum_\alpha x_k^{(\alpha)} \psi_\alpha\left(\theta\right) + S\left(\Delta t, q(\theta), \sum_\alpha x_k^{(\alpha)} \psi_\alpha\left(\theta\right)\right)$$

Applying the Galerkin projection to the equation and using the orthogonality, the following expression is obtained:

$$\forall \beta; \quad x_{k+1}^{(\beta)} = x_k^{(\beta)} + \mathbb{E}\left(S\left(\Delta t, q(\theta), \sum_\alpha x_k^{(\alpha)} \psi_\alpha\left(\theta\right)\right) \psi_\beta(\theta)\right)$$

The last term corresponds to the expected value of the product of the time-stepping-function S and the test function, which can be approximated numerically by a quadrature rule. By doing so, one only has to feed the solver with the proxy model at the previous state calculated at distinct integration points. This allows to run a black box fashion stochastic Galerkin method using the original solver in a sequential manner. For each sequence (time step) the number of solver calls equals the number of integration points in the quadrature rule. It is to be noted that the order of the gPCE extension does not change the number of solver calls. Of course this is only true if the values of time-stepping-function evaluated at the integration points is kept in the memory during calculating all β coefficients. However, for higher order gPCE, higher order quadrature rule should be chosen.

2.2.3 Numerical examples

To test this methodology, it was applied to three different elementary ODE examples of increasing difficulty with stochastic initial conditions:

- Logistic equation:

  $\dot{x} = rx\left(1 - \frac{x}{k}\right)$ $\quad$ x: population

  with r, k model parameters

- The Lotka-Volterra equation, that is, the predator-prey model:

  $\begin{aligned} \dot{x} &= \alpha x - \beta xy \quad && x\text{: number of preys} \\ \dot{y} &= \gamma xy - \sigma y \quad && y\text{: number of predators} \end{aligned}$

  with α, β, γ, σ model parameters

- and the Lorenz 63 equation, the simplified non-linear 'butterfly' model for atmospheric convection:

  $\begin{aligned} \dot{x} &= s(y - x) && x\text{: the rate of convective overturning} \\ \dot{y} &= rx - y - xz && y\text{: horizontal temperature variation} \\ \dot{z} &= xy - bz && z\text{: vertical temperature variation} \end{aligned}$

  with s, r, b model parameters

In the numerical analysis (for all three problems) the time-stepping-function S was a cycle of the ODE solver, namely of the fourth order Runge Kutta explicit time integration scheme. For the three systems only the initial condition was assumed stochastic. In other words, the logistic equation had only one random variable, the predator-prey model two, and the Lorenz equations had three independent random variables. Uniform distribution was assumed for these initial values (x_0, y_0, z_0) and consequently the orthogonal polynomials in the substituting proxi model were Legendre polynomials. Herein different order gPCE was used. The term $\mathbb{E}\left(S\psi_\beta\right)$ was evaluated by applying the Gauß quadrature rule. The expected value was evaluated on the full tensor grid for the multivariate problems. For example the third order gPCE was calculated with four integration points, that is 4, 16 and 64 integration points were used in the logistic, predator-prey and Lorenz equations respectively. As the number of variables grows, the number of quadrature points, that is the number of points where the deterministic solver (the time-stepping-function) has to be evaluated per sequence increases very fast. When the

number of random variables is very high, this number can be reduced by using sparse grids in the quadrature rule. For these small problems herein investigated, even with full tensor grid, the computational cost of the Galerkin method is minor relating to the one of the MC sampling method.

Figures 2, 4 and 6 show the mean of the predicted states of the three systems together with the coloured 3σ region of the stochastic solution. The figures show the results from both the MC brute force calculation with 1 000 000 samples (3σ region in darker colour) and the solutions from the Galerkin method with third order gPCE (3σ region in lighter colour) given above. To be able to see the difference in between the two methods the coloured regions are slightly transparent. In Figure 2 this difference is so small that the mean value of the population and its 3σ region computed with the two different methods visually completely overlap. In the figure the probability distribution function (PDF) at certain time spots are also shown. These PDFs are seperately also shown in Figure 3, where the results received from different order gPCEs are compared.

The logistic model is the most predictable one. Though the uncertainty

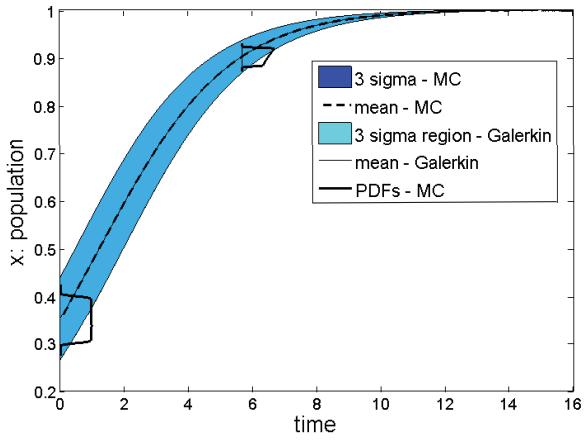

Figure 2: Stochastic logistic equation (50 time steps) - overlapping mean value of population and 3σ region with the Monte Carlo method (10^6 samples) and the Galerkin method (third order gPCE)

grows slightly in the beginning (maximal variance is 20 % higher than the initial one), after time 1.2 the variance is continuously decreasing as the stable attractor at $x = 1$ is approached. For this system even the second order gPCE and quadrature rule with 3 points give acceptable result. The maximal relative error of the variance (relating to the MC simulation) is 1.3% for second order gPCE, which is reduced to 0.3% with third order gPCE. Taking the run time of the 1 000 000 sampled MC simulation as reference, the relative run time of the logistic equation with the Galerkin method with 4 calls per time step (herein 50 time steps) is around 0.22%.

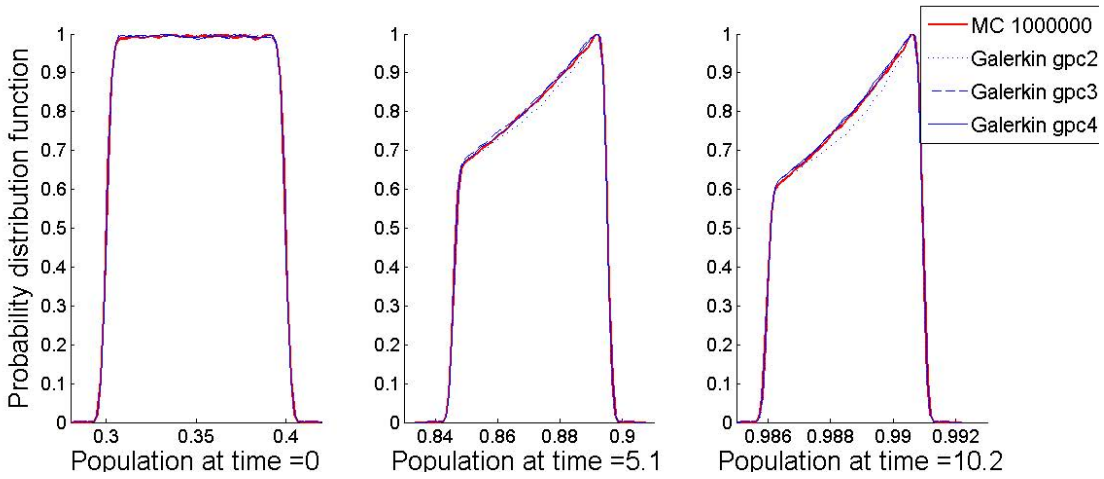

Figure 3: PDFs of the population from the stochastic logistic equation at different time spots with the Monte Carlo method (10^6 samples) and with the Galerkin method using second, third and fourth order gPCE

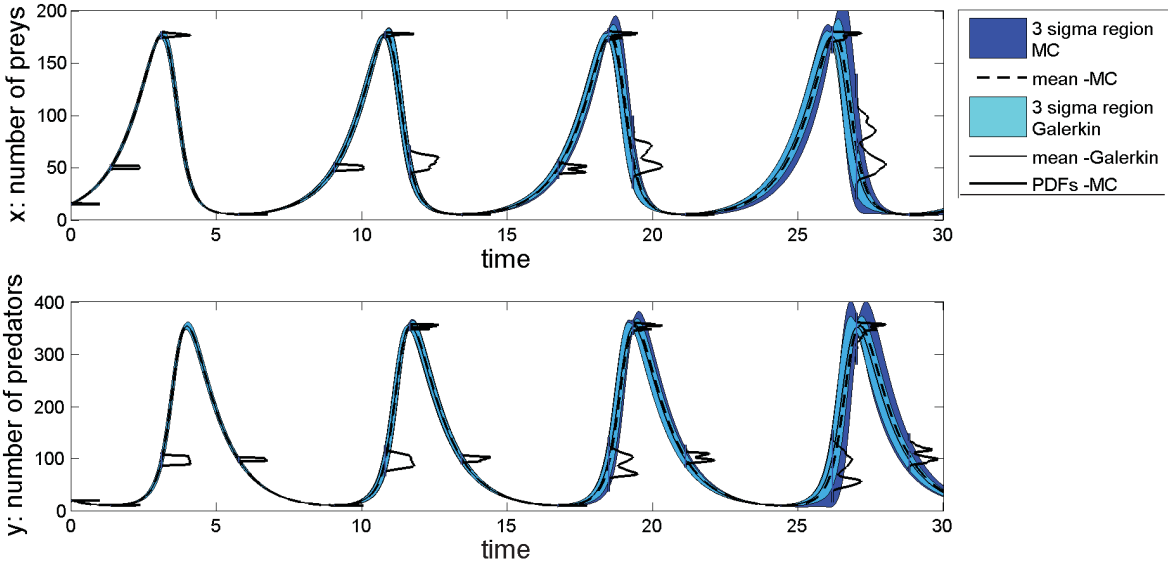

Figure 4: Stochastic Lotka-Volterra equations (100 time steps) - mean value and 3σ region with the Monte Carlo method (10^6 samples) and the Galerkin method (third order gPCE)

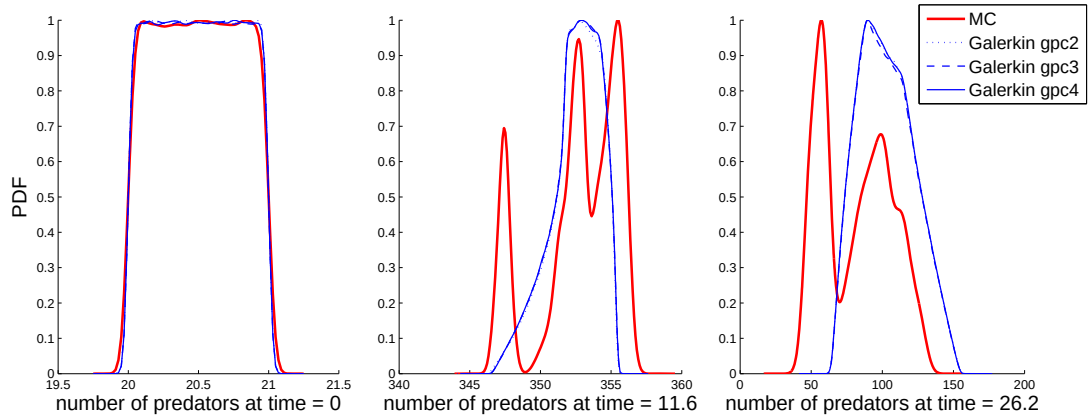

Figure 5: PDFs of the number of predators from the stochastic Lotka-Volterra equations at different time spots with the Monte Carlo method (10^6 samples) and with the Galerkin method using second, third and fourth order gPCE

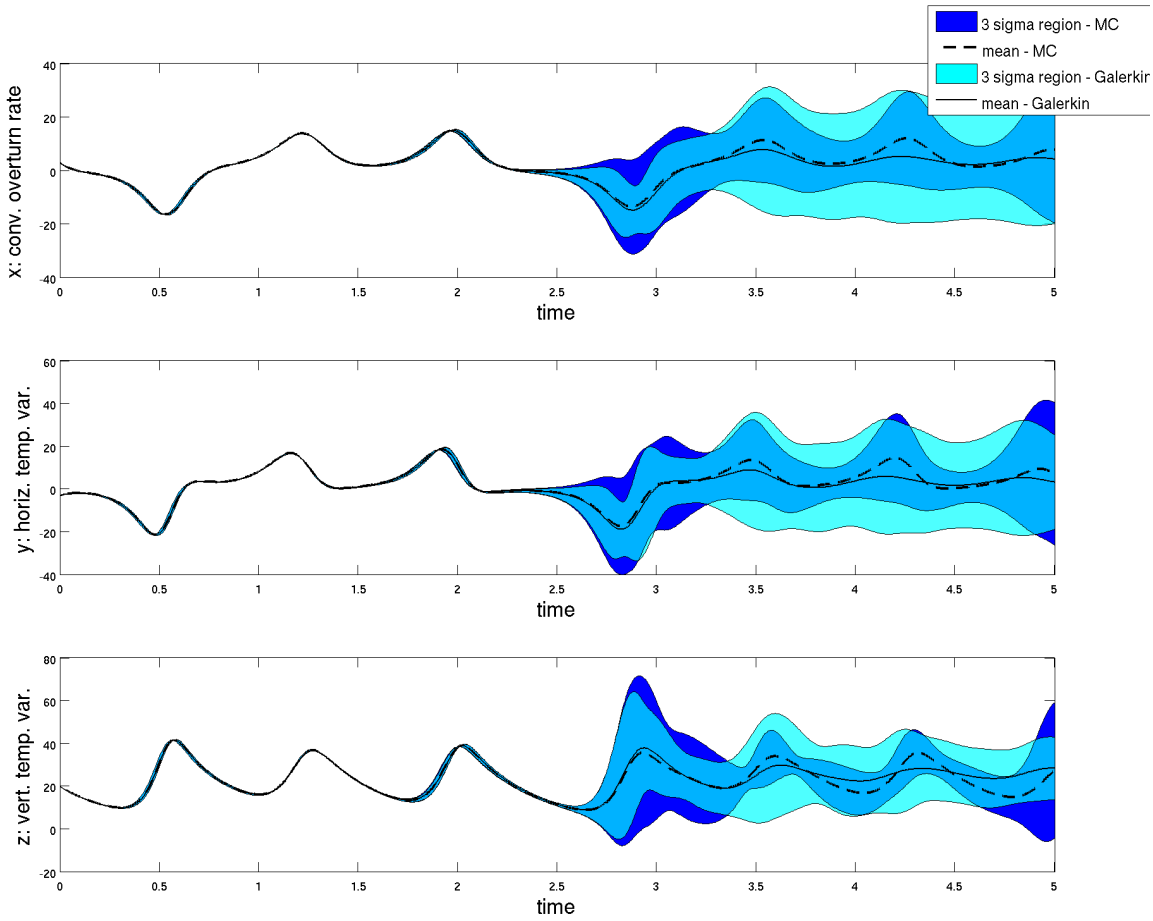

Figure 6: Stochastic Lorenz-63 equations (1000 time steps)- mean value and 3σ region with the Monte Carlo method (10^6 samples) and the Galerkin method (fourth order gPCE)

The other two systems are more educative, in a sense that they demonstrate the sensitivity of the dynamical non-linear systems, and the accumulation of numerical errors as well as the degradation of convergence of the gPCE to the true PDFs. This phenomena arises in the context of long term integration when the given Galerkin method is used. It can be seen on Figures 4, 5 and 6, that with time the uncertainties get more emphasized, the PDFs change to multimodal distributions, and the difference between the methods is much more significant. However, in both examples the characteristic and qualitative behaviour of the systems is well captured. For the predator-prey model, the difference between the mean and variance from the two methods can only be seen at the last peak of the solutions (the region with the lighter colour is the one corresponding to the Galerkin method). This small example takes hours on a PC when run 10^6 times, but for larger systems, even with parallelization, this calculation results in an unaffordable computational burden. In contrast, the offered Galerkin method's evaluation time is around 1%.

Though being a highly simplified model, the Lorenz equations show how unpredictable weather can be. Even a very slight variation of the initial

conditions can completely change the solutions after a few days. Often, for general engineering simulations it is more a qualitative analysis that is needed, to verify for how long it makes sense to predict the model with high accuracy, and the dimension of the corresponding reliability. When the goal is such, the Galerkin method is a competitive method. However, when the task is to identify the true PDFs of the state, more advanced calculation should be implemented. For example, the already proposed time dependent gPCEs [4], or adaptive, piecewise, lower order gPCEs [10] could be tested for the offered algorithm.

References

[1] I. Babuška, F. Nobile, and R. Tempone, *A stochastic collocation method for elliptic partial differential equations with random input data*, SIAM Review **52** (2010), no. 2, 317–355, doi:10.1137/100786356.

[2] R. E. Caflisch, *Monte Carlo and Quasi-Monte Carlo methods*, Acta Numerica **7** (1998), 1–49, doi:10.1017/S0962492900002804.

[3] P. G. Constantine, M. S. Eldred, and E. T. Phipps, *Sparse pseudospectral approximation method*, Computer Methods in Applied Mechanics and Engineering **229-232** (2012), 1–12, doi:0.1016/j.cma.2012.03.019.

[4] M. Gerritsma, J.-B. van der Steen, P. Vos, and G. Karniadakis, *Time-dependent generalized polynomial chaos*, Journal of Computational Physics **229** (2010), 8333–8363, doi:10.1016/j.jcp.2010.07.020.

[5] R. G. Ghanem and P. D. Spanos, *Stochastic finite elements: A spectral approach*, Dover Civil and Mechanical Engineering, Dover Publications, 2012.

[6] L. Giraldi, A. Litvinenko, D. Liu, H. G. Matthies, and A. Nouy, *To be or not to be intrusive? The solution of parametric and stochastic equations - the "plain vanilla" Galerkin case*, 2013, URL: http://arxiv.org/abs/1309.1617.

[7] H. G. Matthies, *Uncertainty quantification with stochastic finite elements*, John Wiley and Sons, 2007, doi:10.1002/0470091355.ecm071.

[8] G. Migliorati, F. Nobile, E. von Schwerin, and R. Tempone, *Analysis of discrete ℓ_2 projection on polynomial spaces with random evaluations*, Foundations of Computational Mathematics (2014), doi:10.1007/s10208-013-9186-4.

[9] M. Papadrakakis and V. Papadopoulos, *Robust and efficient methods for stochastic finite element analysis using Monte Carlo simulation*, Computer Methods in Applied Mechanics and Engineering **134** (1996), 325–340, doi:10.1016/0045-7825(95)00978-7.

[10] X. Wan and G. E. Karniadakis, *An adaptive multi-element generalized polynomial chaos method for stochastic differential equations*, Journal of Computational Physics **209** (2005), no. 2, 617–642, doi:10.1016/j.jcp.2005.03.023.

[11] D. Xiu and G. Karniadakis, *The Wiener–Askey polynomial chaos for stochastic differential equations*, SIAM Journal on Scientific Computing **24** (2002), no. 2, 619–644, doi:10.1137/S1064827501387826.

2.3 Centre of Scientific Computing

Ansprechpartner:	Thorsten Grahs
EMail:	t.grahs@tu-bs.de
Telefon:	0531/391-3008

The Centre of Scientific Computing (CSC) is a joint research centre of the Institutes of Scientific Computing (Prof. Matthies) and Computational Mathematics (Prof. Sonar) within the Innovationsgesellschaft TU Braunschweig (iTUBS). The purpose of the centre is consulting and project management for problems from applied mathematics and scientific computing

2.3.1 Work carried out

In 2013 several research and industrial projects were carried out. Furthermore, various training courses concerning the simulation tool-box OpenFOAM have been conducted, both in Braunschweig as well as at the customer site.

Projects

- **GPGPU-accelerated simulation of water-wading of a car using Lattice-Boltzmann-Methods (LBM)**
  Research partner: Volkswagen AG
  joined work with Dr.-Ing. Ch. Janßen, Fluid Dynamics and Ship Theory, TU Hamburg-Harburg
- **Feasibility study for the reconstruction of the inner and outer part of the Mercury magnetic field**
  Research partner: Inst. f. Geophysik und Extraterristische Physik
  further implementation of the project from 2012.
- **Validation of numerical simulations for marine Geometries**
  Research partner: Schottel
  Simulation of
  - the Potsdam Propeller Test Case (PPTC)
  - the Korean Container Ship (KCS) test case.

Talks

- Janßen, C. and Grahs, T., *High performance computing on General Purpose Graphical Processing Units for innovative automotive application.* «««< .mine Proc. of the NAFEMS Seminar Innovative

Applications of Computational Fluid Dynamics (CFD) in Product Development. March 2013. ======= Proc. of the NAFEMS Seminar "Innovative Applications of Computational Fluid Dynamics (CFD) in Product Development". March 2013. »»»> .r3881

- Janßen, C. and Grahs, T, *High performance computing on General Purpose Graphical Processing Units for innovative automotive application.* Proc. of the NAFEMS Seminar "Innovative Applications of Computational Fluid Dynamics (CFD) in Product Development". March 2013.

Training courses

- OpenFOAM introduction
  March, September and December, TU Braunschweig
- OpenFOAM advanced
  March and September 2013, TU Braunschweig
- Customized on-site training courses (customer site)
  - Schottel AG, 29. – 30.10.2013
  - TU Dresden, 12. – 16.08.2013

Workshop organisation

- **NOFUN 2013** – Northern germany OpenFoam User MeetiNg
  Braunschweig, Haus d. Wissenschaften, 9.10.2013
  With participants from DLR, FH Kiel, TU Berlin, TU Hamburg-Harburg, TU Braunschweig, Chalmers University Gothenburg, FutureShip, Engysy, ...

2.4 Uncertainty Quantification for a Preliminary CESTOL Aircraft Design

Ansprechpartner:	Noémi Friedman, Martin Krosche, and Bojana Rosić
EMail:	n.friedman@tu-bs.de, martin.krosche@tu-bs.de
Telefon:	0531/391-3013, 0531/391-3012

The collaborative research centre (CRC) 880 is concerned with fundamentals of high lift for a new kind of low noise cruise efficient civil aircraft which enables short take-off and landing (CESTOL). New technologies are handled through a mutual exchange of incremental progress among the projects of the CRC 880. Our task is to model and analyse the uncertainties which come along with the new technologies; these uncertainties are mostly epistemic. The uncertainty analysis is performed for a deterministic preliminary reference design of an appropriate CESTOL aircraft and is based on stochastic formulations.

Section 2.4.1 outlines new achievements in the robustness analysis of the reference design, which involves surrogate models described through small sets of stochastic polynomials. Section 2.4.2 focuses on the enhancement of the maneuverability analysis of the aircraft design through uncertainty quantification of the flight dynamics simulation model. A model simulating a conventional turbo propeller engine driven aircraft (Basic Aircraft Model) is analysed in a purely non-intrusive manner. In the next project phase these findings will be updated to quantify uncertainties in the simulation model adapted to the CESTOL aircraft design.

2.4.1 Robustness Analysis on the Basis of Surrogate Models in Sparse Representations

For a robustness analysis the deterministic reference CESTOL aircraft design is extended through a stochastic formulation of parameter variations, which results in a probabilistic model. A robustness analysis via a basic Monte Carlo (MC) sampling is published in [5, 4]; many expensive samples of the probabilistic model were required to obtain statistics of acceptable accuracy. In addition to the MC sampling, a surrogate model for the probabilistic model is determined in [4]. There, the surrogate model is represented by a truncated polynomial chaos expansion (PCE) with a basic set of Legendre polynomials defined in uniformly distributed random variables; the coefficients are computed through a least squares regression approach [1] using MC samples. It turned out that the surrogate model requires far fewer samples than basic MC sampling to obtain statistics of the same accuracy. In addition, many terms in the PCE do not carry an essential content of information, so that they

could be neglected to obtain a computationally more efficient surrogate model.

As a consequence, the main motivation of this year was to adaptively find a small set of stochastic polynomials for representing a surrogate model without any essential loss of accuracy. For this purpose the adaptive algorithm in [2] is used, which is based on the mentioned least squares regression approach. The algorithm iteratively performs forward and backward steps, in which new stochastic polynomials are added or deleted one-by-one to estimate the content of information which is carried by their corresponding terms of the PCE; however, each addition — and also usually each deletion — is linked to solving a linear system. Thus, for performance reasons the system should always be as small as possible, which exactly corresponds to a sparse PCE — that is a PCE with a small set of stochastic polynomials. When the system is growing due to the addition of stochastic polynomials, more samples are generally required. In [6] a proportionality relation is given between the number of stochastic polynomials and the number of samples, needed to obtain convergence. This relation is used here to choose the number of sample points a priori when stochastic polynomials are added or deleted. The convergence for the described algorithm is shown in Fig. 7 for different design parameters of the aircraft and the maximum norm over the considered twenty-one output design parameters. It is obvious that few stochastic polynomials are enough to obtain a description of acceptable accuracy.

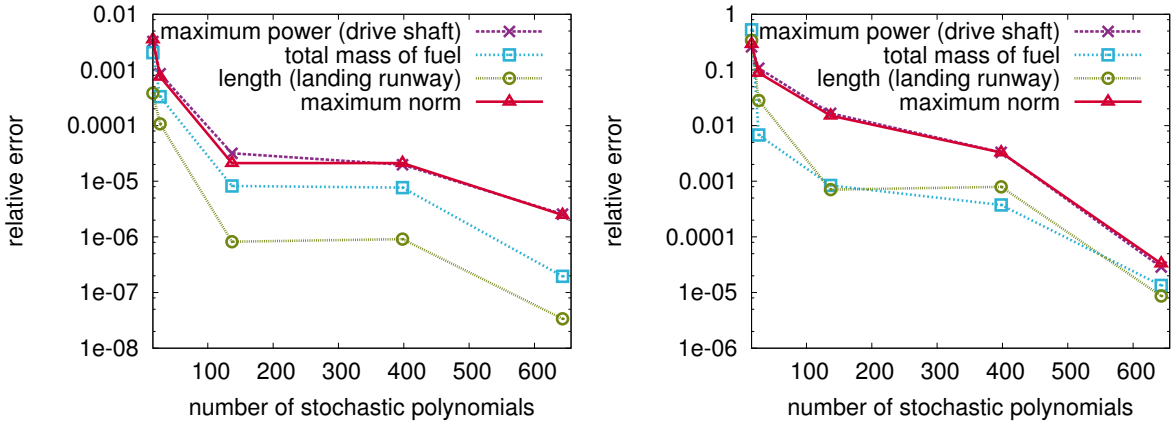

Figure 7: Convergence of the expectation of some output parameters in Fig. (a) and their variance in Fig. (b) according to the number of stochastic polynomials chosen to obtain a PCE of higher accuracy.

Another question is if the coefficients can be compressed so that an accurate low-rank representation for the surrogate model can be obtained. To get an idea about the answer the Karhunen Loève Expansion (KLE) is determined for a surrogate model which was computed by the least squares regression approach taking into account all samples from

the basic MC run. Fig. 8 displays the decline of the eigenvalues of the KLE and the convergence of the variance of some design parameters according to the number of terms used in the KLE. Because of the chosen scaling of the parameters the discrepancy between a fast decline of the eigenvalues and a slow convergence of at least some parameters arises.

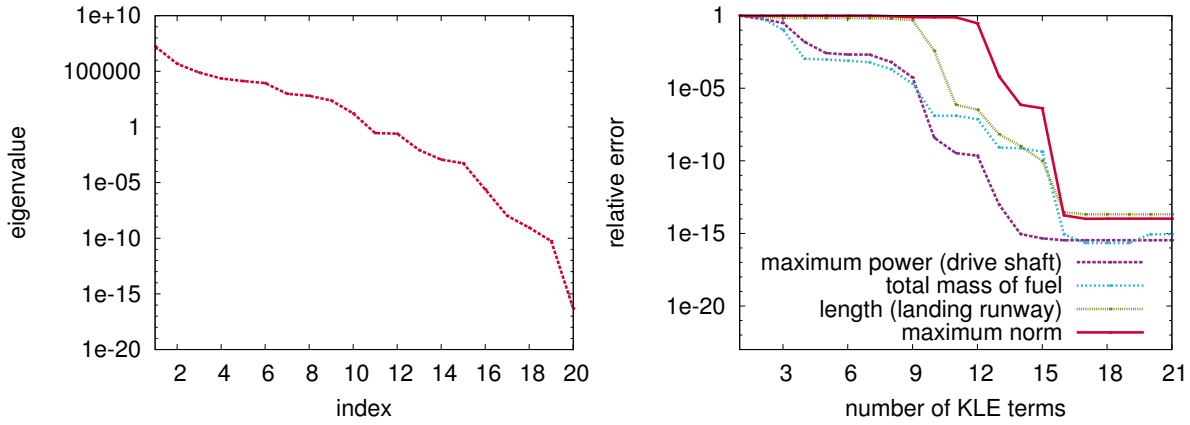

(a) (b)

Figure 8: Decline of the eigenvalues in Fig. (a) and convergence of the variance of some output parameters according to the number of terms used in the KLE.

2.4.2 Uncertainty quantification of a non-linear dynamic simulation model

Extremely high lift along with low dynamic pressure place high demands on the trim and controllability of the analyzed CESTOL aircraft. In order to be able to reliably test maneuverability of the aircraft, one has to carry out its stochastic aerodynamic analysis. The main focus of this project is to enhance the reliability of the CESTOL model by quantifying its uncertainties, that is, to analyse the aircraft behaviour under the influence of uncertainties of its input parameters. Herein a preliminary analysis of a model simulating a similar turbo propeller engine driven aircraft (Basic Aircraft Model) is carried out in parallel with the development of the new simulation model adapted for the CESTOL aircraft design. As the two models are of similar properties, the outlined methodology can be easily updated to the new model. The stochastic analysis is accomplished in a non-intrusive manner, meaning that the original model is treated in a black box fashion.

The numerical investigation is carried out for the aircraft example in an unaccelerated horizontal flight initiated by a elevator pulse at time $t = 1$ [s], see Fig. 9 and [3] for the deterministic description of the model. In this plot the typical peaks of the well known phugoid motion, e.g. trajectories of angle of attack (AoA) (α), pitch rate (q), pitch attitude (θ), altitude (h) and true air speed (V_{TAS}), can be seen. The uncertainties are assumed to be present in the description of the aerodynamics, for more information please see [8, 7]. Note that these uncertainties originate from

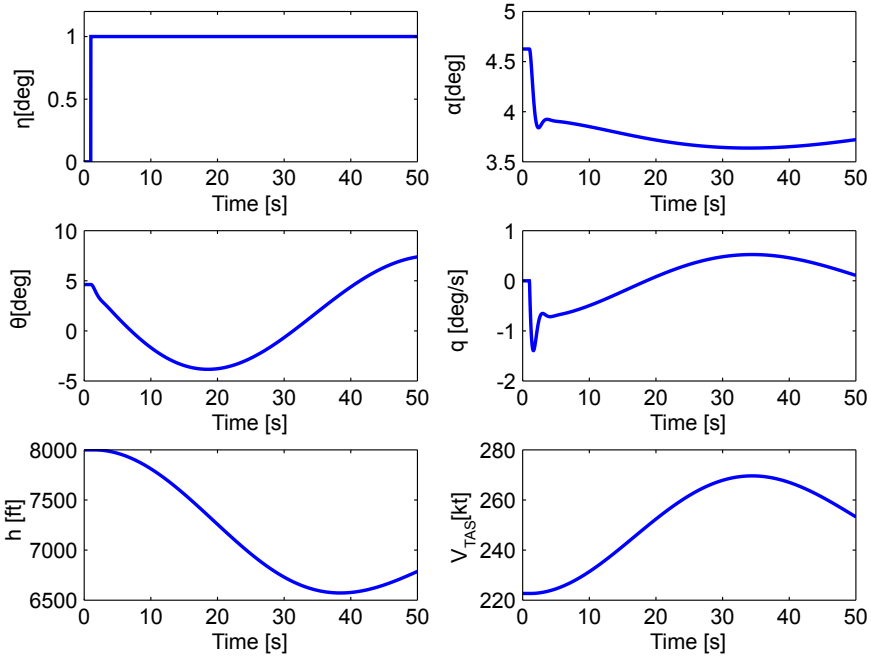

Figure 9: The excitation and response of the aircraft model

the model error, and hence do not represent the parameter nature. This assumption results in the random aircraft phugoid motion represented by many possible trajectories. To clarify this, the mean altitude trajectories together with the 99% confidence intervals and corresponding probability density functions are shown in Figs. 10. According to these plots, the uncertainty of the altitude is initially small, and hence the PDF is narrowed, i.e. almost deterministic. However, after the system is initiated by the elevator pulse the uncertainty starts increasing over time until $t = 40$ [s]. In this moment the 99% region has maximal extent and the uncertainty starts decreasing.

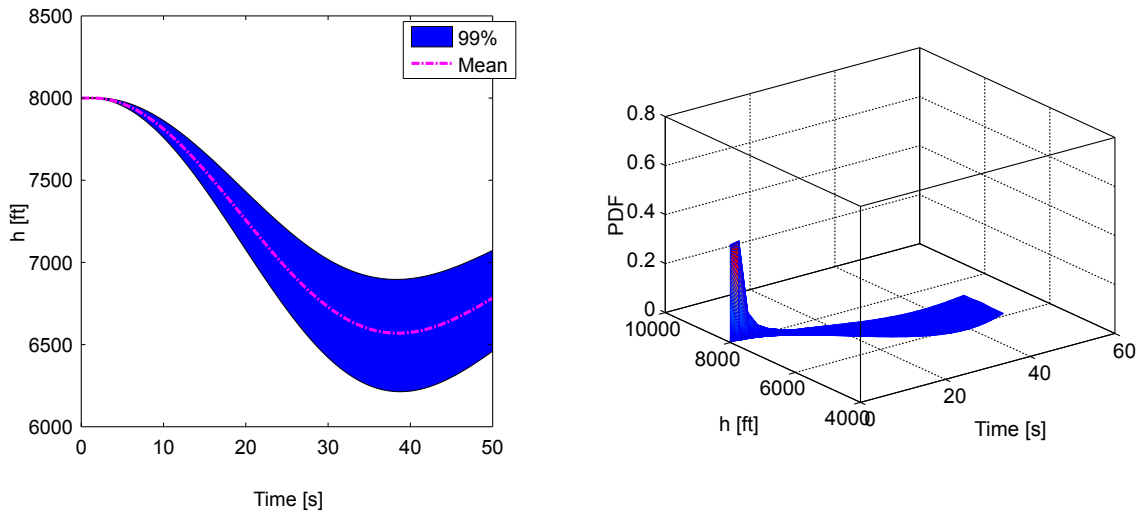

Figure 10: Random altitude trajectory

Table 1: Comparison of the first sensitivity Sobol' index obtained by polynomial chaos (PCE) and Monte Carlo (MC) approaches

Index	θ [deg]	α [deg]	h [ft]	q [deg/s]	V_{TAS} [kt]
PCE	0.1902	0.3477	0.2126	0.2797	0.2188
MC	0.1887	0.3481	0.2099	0.2773	0.2160

Once the uncertainties are quantified, one may compare the modified coefficients of variation (the ratios of the standard deviation to the maximum of the mean) for different aircraft response characteristics as presented in Fig. 11. The comparison shows that the uncertainty in the pitch attitude grows up to circa 10%, while the second largest deviation belongs to the pitch rate, as expected. The least uncertain is the angle of attack whose coefficient of variation is much smaller than 1%.

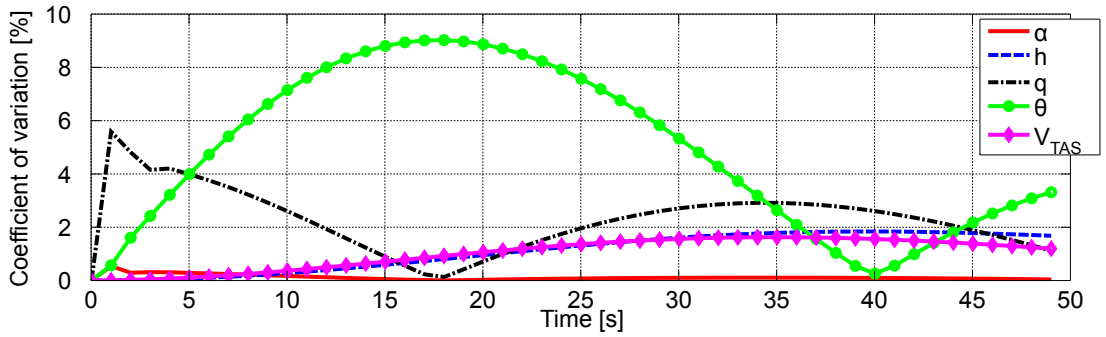

Figure 11: The coefficient of variation for the aircraft response characteristics: α- the angle of attack, h - the altitude, q - the pitch rate, θ- the pitch attitude and V_{TAS} - the true airspeed

The variance-based sensitivity analysis of the system behaviour on the input uncertainty is investigated with the help of the Sobol' sensitivity theory, see [8]. The first sensitivity index of the output response due to the uncertainty in the lift coefficient is computed with the help of Monte Carlo simulation with 100 000 samples, as well as the polynomial chaos theory, please see Tab. 1. These findings indicate that the lift coefficient has the greatest impact on the angle of attack, which agrees with the theoretical assumptions. Additionally, the comparison analysis provided in Tab. 1 shows that that both sensitivity indices match on the second decimal. This corresponds to the accuracy of the Monte Carlo simulation.

Now, in the next phase of the project, the methodology is being updated to the new simulation model which incorporates the active high lift system of the CESTOL design. In parallel, enhancement of the stochastic model with non-intrusive Galerkin method (see Section 2.2) and addition of new polynomials are planned.

References

[1] M. Berveiller, B. Sudret, and M. Lemaire, *Stochastic finite element: A non intrusive approach by regression*, European Journal of Computational Mechanics **15** (2006), no. 1–3, 81–92.

[2] G. Blatman and B. Sudret, *Sparse polynomial chaos expansions and adaptive stochastic finite elements using a regression approach*, Comptes Rendus Mécanique **336** (2008), no. 6, 518–523, doi:10.1016/j.crme.2008.02.013.

[3] J. H. Diekmann and K.-U. Hahn, *Nonlinear flight dynamics simulation model for a civil aircraft with active high lift system*, SFB 880 - Fundamentals of high-lift for future commercial aircraft (R. Radespiel and R. Semaan, eds.), TU Braunschweig - Campus Forschungsflughafen, 2013.

[4] M. Krosche, *A generic component-based software architecture for the simulation of probabilistic models*, Ph.D. thesis, Technische Universität Braunschweig, Braunschweig, 2013, http://www.digibib.tu-bs.de/?docid=00052792.

[5] M. Krosche and W. Heinze, *An aircraft design with uncertain parameters: A robustness analysis through a component-based software system*, SFB 880 — Fundamentals of High-Lift for Future Commercial Aircraft, Biennial Report, CFF Forschungsberichte, no. 2013–03, TU Braunschweig — Campus Forschungsflughafen, Braunschweig, 2013, pp. 191–203.

[6] G. Migliorati, F. Nobile, E. von Schwerin, and R. Tempone, *Analysis of the discrete L^2 projection on polynomial spaces with random evaluations*, Mox-report no. 46, Dipartimento di Matematica, Politecnico di Milano, Milano, 2011, http://mox.polimi.it/it/progetti/pubblicazioni/quaderni/46-2011.pdf.

[7] B. Rosić and J. Diekmann, *Non-intrusive methods for the uncertainty quantification of basic aircraft model (bacm)*, SFB 880 – Fundamentals of High-Lift for Future Commercial Aircraft, Biennial report (R. Radespiel and R. Seman, eds.), TU Braunschweig- Capmus Forschungsflughafen, 2013, pp. 204–216.

[8] B. Rosić and J. Diekmann, *Stochastic description of aircraft simulation models and numerical approaches*, Tech. Report 2014-01, Institute of Scientific Computing, Technische Universität Braunschweig, 2014, URL: http://www.digibib.tu-bs.de/?docid=00055749.

2.5 The nonlinear Bayesian update

Ansprechpartner:	Alexander Litvinenko
EMail:	litvinen@tu-bs.de,
	alexander.litvinenko@kaust.edu.sa
Telefon:	0531/391-3008

The following results are published in [1]. In this work the algorithm developed by Elmar Zander (please also refer to his report below) is used to compute non-linear Bayesian update ingredients. This work is also prolongation of work done in [2, 3, 4]. Further we demonstrate

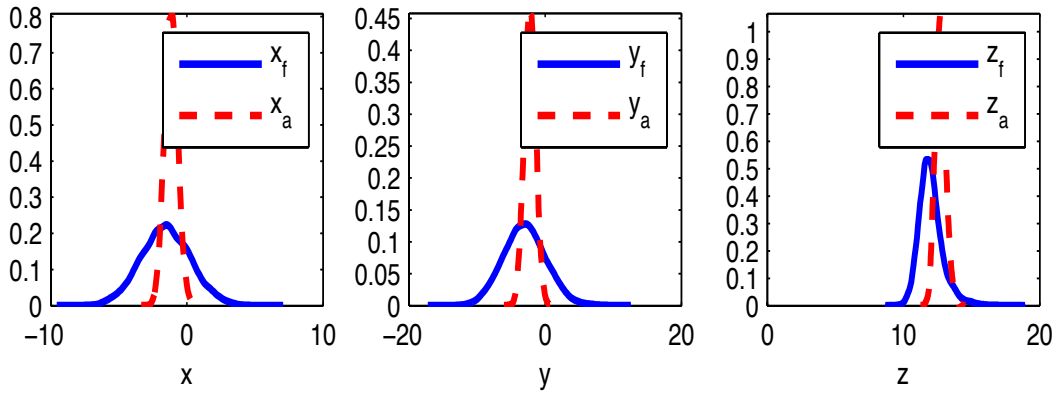

Figure 12: Linear measurement: prior and posterior after one update

a quadratic ($n = 2$) Bayesian Update computation. The case $n > 2$ can be done similarly (see [1] and report of Elmar Zander below). We consider the example of the chaotic Lorentz-84 [2] model. For this kind of experiment it has several advantages: it has only a three-dimensional state space, these are the uncertain 'parameters', i.e. $(x, y, z) \in \mathcal{Q} = \mathbb{R}^3$, the system is sufficiently nonlinear to make the problem difficult, and adding to this we operate the equation in its chaotic regime, so that new uncertainty is added between measurements.

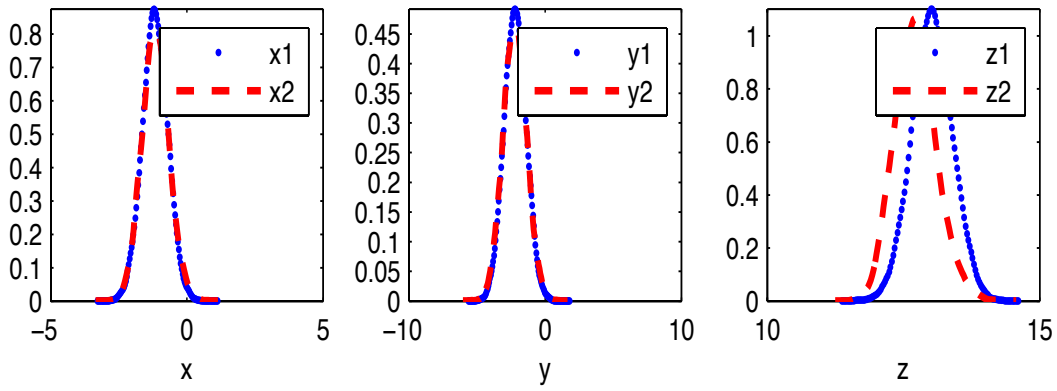

Figure 13: Linear measurement: Comparison posterior for LBU ($n = 1$) and NLBU ($n = 2$) after one update

As a first set of experiments we take the measurement operator to

be linear in parameter q; $Y(q) = q = (x, y, z)$, i.e. we can observe the *whole* state directly. At the moment we consider updates after each day. See more pictures in [2], where the updates were performed every 10 days. The results for the pdfs of the state variables are shown in Fig. 12, where the prior and the posterior pdf for a LBU after one update are given (index f - forecast, prior; index a - assimilated, posterior). Then we do the same experiment, but with a *quadratic* nonlinear BU (NLBU) with $n = 2$. The results for the posterior pdfs are given in Fig. 13, where the linear update (index a) is dotted in blue, and the full red line is the quadratic NLBU; there is hardly any difference between the two, except for the variable z. If we go on to the second update—after two days—some differences appear, the results for the posterior pdfs are in Fig. 14.

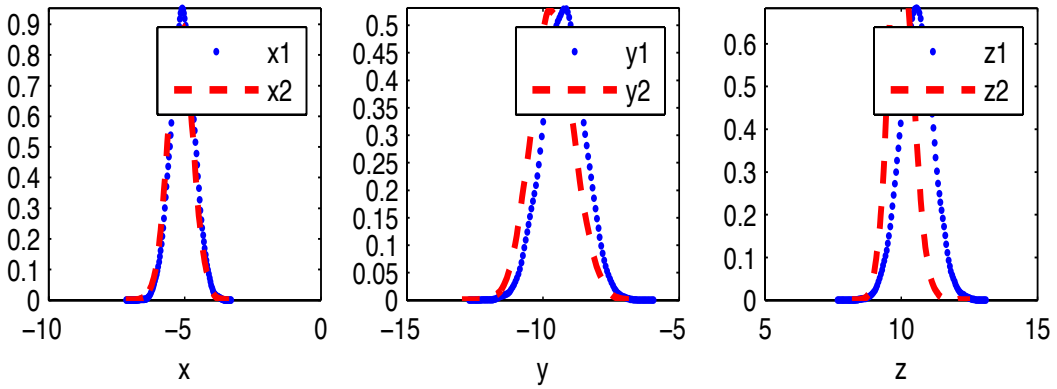

Figure 14: Linear measurement: Comparison posterior for LBU ($n = 1$) and NLBU ($n = 2$) after second update

As the differences between LBU and NLBU with $n = 2$ were small—we take this as an indication that the LBU is not too inaccurate an approximation to the conditional expectation—we change the experiment and take a nonlinear measurement function, which is now cubic: $Y(q) = (x^3, y^3, z^3)$. We now expect larger differences between LBU and NLBU.

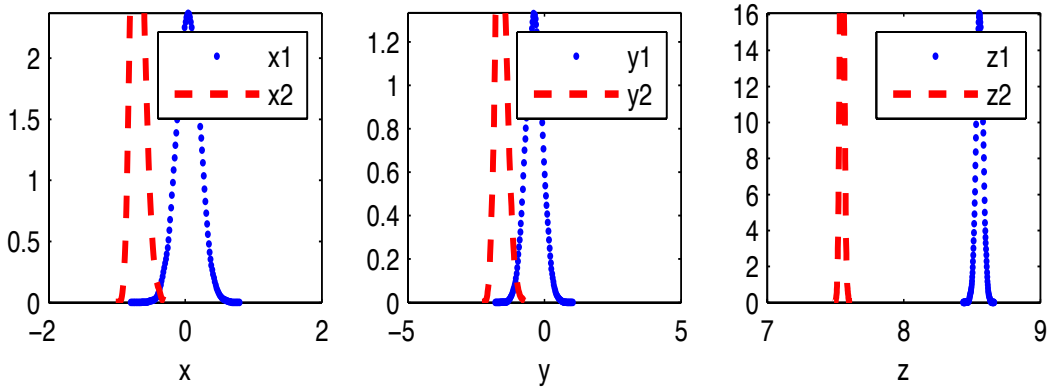

Figure 15: Cubic measurement: Comparison posterior for LBU ($n = 1$) and NLBU ($n = 2$) after one update

These differences in posterior pdfs after one update may be gleaned from Fig. 15, and they are indeed larger than in the linear case Fig. 13, due to the strongly nonlinear measurement operator.

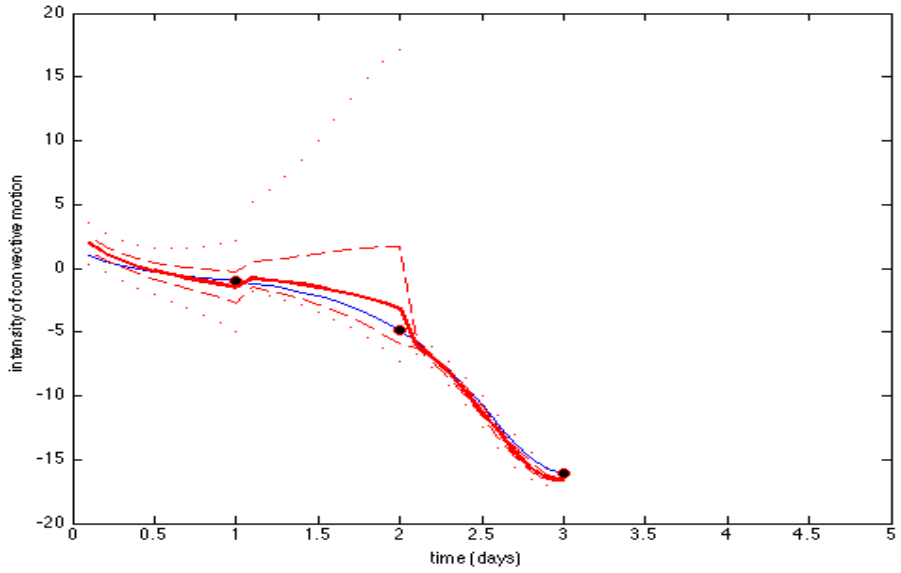

Figure 16: Partial state trajectory with uncertainty and three updates

As the cubic is quite a strong nonlinearity, we performed a set of experiments where the measurement function is $Y(q) = (x|x|, y|y|, z|z|)$; only a quadratic nonlinearity, but no loss of information about the sign. Fig. 16 shows the trajectory of one state variable (the updates are performed every day).

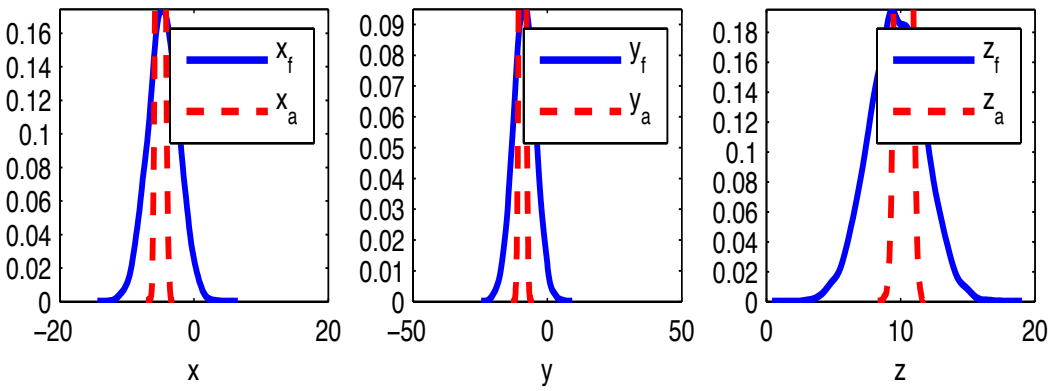

Figure 17: Quadratic measurement: Comparison posterior for LBU ($n = 1$) and NLBU ($n = 2$) after one update

The results for the 2-nd update are displayed for the posterior pdfs in Fig. 17. This has to be compared Fig. 14, and the differences are indeed much larger, but smaller than in Fig. 15.

References

[1] A. Litvinenko and H. G. Matthies, *Inverse problems and uncertainty quantification*, Tech. report, arXiv:1312.5048, 2013.

[2] O. Pajonk, B. Rosić, A. Litvinenko, and H. G. Matthies, *A deterministic filter for non-Gaussian Bayesian estimation*, Physica D: Nonlinear Phenomena **241** (2012), no. 7, 775–788, doi:10.1016/j.physd.2012.01.001.

[3] B. Rosić, A. Kučerová, J. Sýkora, O. Pajonk, A. Litvinenko, and H. G. Matthies, *Parameter identification in a probabilistic setting*, Engineering Structures, availible online (2013), doi:10.1016/j.engstruct.2012.12.029.

[4] B. Rosić, O. Pajonk, A. Litvinenko, and H. G. Matthies, *Sampling-free linear bayesian update of polynomial chaos represenations*, Journal of Computational Physics **231** (2012), no. 17, 5761–5787.

2.6 A Selection of CTL-based Parallel Algorithms

Ansprechpartner:	Rainer Niekamp
EMail:	r.niekamp@tu-braunschweig.de
Telefon:	0531/391-3010

The Component Template Library (CTL) is a light weight implementation of the software component technology which separates strongly the parts of an application into components, where these components interact only via their interfaces. The main aspects, which are the basis for the design of the CTL are

- covering the features of the programming language C++
- simple handling
- maximum de-coupling of the CTL components
- run time efficiency
- flexible employment of existing components.

These design goals were reached by using the Meta Template programming, with the introduction of abstract data types and by a simple efficient protocol as well as by the availability of a number of of communication/connection variants.

The CTL has been successfully applied in computational applications like multi-physics simulation [1, 2, 8, 11, 10], multi-scale simulation [9, 5], stochastic finite element analysis [4, 3] and optimisation [6].

Often a component based application is given by a set of client/server connections, where each server is owned and instantiated by its client. But this topology does not support efficiently parallel applications. For this purpose the CTL provides an implementation of the process group concept. As of version 2.1 the CTL supports this concept for all reasonable protocols which are tcp/ip, mpi, pvm and thread. A group is a set of run-time components, where each member has a connection/link to each other. Similar to an MPI-group each member has a rank, by which the corresponding link can be addressed. Features of `ctl::group` are

- external and internal groups
- usage of internal groups
  - MPI based implementation by dynamic MPI allocation
  - broadcast and merge operators in internal group

  - asynchronous algorithms: evaluate, run(), run(synchron functor)

- usage of external groups
  - MPI based implementation by static MPI groups or MPI application schemes
  - support of remote or distributed objects like vector, matrix

A group provides complete connectivity of the components and is therefor useful to realise parallel algorithms, either on a cluster using the mpi, pvm or tcp protocol or on the cores of a multi-core CPU using the thread protocol. For the usage of groups, please see in the CTL examples:
http://www.wire.tu-bs.de/forschung/projekte/ctl/e_ctl.html
==> Downloads ==> CTL version 2.1
After the download you will find the directory `ctl/examples2/group`.

2.6.1 Loop Parallisation

In the case where operations performed in a loop are completely independent they can be evaluated in parallel. The Open Multi-Processing (OpenMP) standard supports an automatic parallelisation on a multi-core CPU for such loops. The following example compares the efficiency of `ctl::evaluate` and OpenMP loop parallelisation.

```
// The ctl::evaluate needs a class for remote invocation
struct functor
{
  int operator()(double x) const
  { // do some work
    for(int i=0; i<1000; i++)
      x *= sqrt(1.0+i);
    return x;
  }
} f;

void test1(const ctl::vector<double>& x)
{
  CTL_Profile("ctl::test");
// unaryCI is a predefined template CI for unary functors
  typedef functorCI::unaryCI<int, double> unaryCI;
  const size_t nWorker=7;
// reduce latency: hire on each thread each worker twice
  ctl::vector<unaryCI> worker(2*nWorker+1);
  for(size_t i=0; i<nWorker; i++)
    worker[i+nWorker] = worker[i] = unaryCI(f, ctl::thread);
// hire yourself once, in order to have some work in this thread
  worker[2*nWorker] = unaryCI(f, ctl::lib);
// call evaluate with a reasonable chunksize
  ctl::vector<int> y=ctl::evaluate<int>(worker, /*data*/x, /*chunksize*/10000);
}
```

```
void test2(const ctl::vector<double>& x)
{
  CTL_Profile("omp::test");
  ctl::vector<int> y(x.size());
#pragma omp parallel for
  for(size_t i=0; i<x.size(); i++)
    y[i] = f(x[i]);
}
void test3(const ctl::vector<double>& x)
{
  CTL_Profile("ref::test");
  ctl::vector<int> y(x.size());
  for(size_t i=0; i<x.size(); i++)
    y[i] = f(x[i]);
}
int main(int n, char **arg)
{
// produce a rather large vector with arbitrary content
  ctl::vector<double> x(10*1000*1000);
  for(size_t i=0; i<x.size(); i++)
    x[i] = 1.0/(2.0+i);
  test1(x);  test2(x);  test3(x);
  return 0;
}
```

The CTL-profiler, activated by the macro `CTL_Profile` generates following output

```
** in ctl::test ** spent time:   14 sec due to  1 call(s) (1.396e+01 sec/call)
** in omp::test ** spent time: 13.8 sec due to  1 call(s) (1.377e+01 sec/call)
** in ref::test ** spent time:  110 sec due to  1 call(s) (1.098e+02 sec/call)
```

The third argument of `ctl::evaluate`, namely the `chunksize`, determines the granularity of the communication with the `workers`, i.e. the size of the data given in each invocation. The parallel efficiency using `ctl::evaluate` is here $\frac{110}{8*14} = 0.982$ and using OpenMP we get $\frac{110}{8*13.8} = 0.996$. In the case of using local threads only, one can not do better than using OpenMP which is part of the compiler, but on the other hand the CTL version is free to hire other workers on other processors, please see also: `ctl/examples2/vectorise`

2.6.2 Distributed Remote Objects

The following example code, see `ctl/examples2/distributedVector`, creates remote objects on an external group. All operations are performed remotely in parallel. The constructor of `algebraCI::vectorCI` distributes the data onto the group members. The distributed instances of the vectorCI's keeping corresponding entries of the data, live on the same thread and there they can communicate locally, which leads to efficient parallel execution of the binary operators like addition.

```
// let algebraCI live on a mpi-group with master connected to THIS process via pipe
// dvector.mpi is an mpi application scheme
// dvector.ctl.exe implements the distributed vector algebra
  algebraCI::use( ctl::link("./dvector.mpi bin/dvector.ctl.exe -l pipe") );

// create a vector and give it to the distributed vector template algebraCI::vectorCI
  double dat[10] = { 3.0, 3.1, 3.2, 3.3, 3.4, 3.5, 3.6, 3.7, 3.8, 3.9 };
  ctl::vector<double> v(&dat[0], &dat[10]);

// perform some distributed remote operations
  algebraCI::vectorCI<double> V(v), W = 9.0*V, S=V+W;
  double sw=S.scal_mult(W);

// get now the sampled data for output
  ctl::vector<double> w=W.getData(), s=S.getData();
  std::cout << "V = " << v << "\n";
  std::cout << "W := 9 * V = " << w << "\n";
  std::cout << "S := V+W = " << s << "\n";
  std::cout << "<S, W>  = " << sw << "\n";
```

This produces the expected output. Please observe that the syntax using these parallised algebraic operators is exactly as in the serial case, where as here the operations `W = 9.0*V, S=V+W` are executed remotely and generate distributed vector instances without communicating the entries of the vectors themselves. For access of the interface `algebraCI::vectorCI` provides the method `getData()`.

2.6.3 Asynchronous Parallel Recursion

The asynchronous parallel algorithms defined by the template `ctl::asynchron` might be used as in the following very academic example:

```
// fibonacci(n) = fibonacci(n-1) + fibonacci(n-2)
// fibonacci(0) = fibonacci(1) = 1
class fibonacci: public ctl::asynchron<fibonacci, int, int>
{
  typedef ctl::asynchron<fibonacci, int, int> baseT;
  int resM[2];
public:
// start fibonacci recursion given above
  fibonacci(int n)
  {
    CTL_Profile("fib");
    resM[0] = resM[1] = 0;
    if(n<2) // trivial case
      resM[0] = 1;
    else // recursive call
    {
// remote call with index 0
      baseT::call<fibonacci>(n-1);
// local call with index 1
      baseT::callLocal<fibonacci>(n-2);
```

```
    }
  }
// set final result here
  ~fibonacci()
  { baseT::set(resM[0] + resM[1]); }
// receive partial results
  void operator()(int res, ctl::uint8 index)
  { resM[index] = res; }
};
// start asynchron recursion by
  CTL_Profile("all");
// starting an internal group of total size 8
  ctl::group G( ctl::location("bin/fibonacci.ctl.exe -l tcp -n 7") );
// invoke the corresponding group::run instance
  int res = G.run<fibonacci>(25);
  std::cout << "fibonacci(25) = " << res << "\n";

output:
fibonacci(25) = 121393
 ** in all ** spent time: 1.69 sec due to     1 call(s) (1.691e+00 sec/call)
 ** in fib ** spent time: 1.12 sec due to 31471 call(s) (3.572e-05 sec/call)
 ** in fib ** spent time: 1.12 sec due to 30950 call(s) (3.614e-05 sec/call)
 ** in fib ** spent time: 1.14 sec due to 30602 call(s) (3.735e-05 sec/call)
 ** in fib ** spent time: 1.03 sec due to 29863 call(s) (3.463e-05 sec/call)
 ** in fib ** spent time: 0.98 sec due to 29494 call(s) (3.318e-05 sec/call)
 ** in fib ** spent time: 1.02 sec due to 26978 call(s) (3.765e-05 sec/call)
 ** in fib ** spent time: 1.08 sec due to 30106 call(s) (3.588e-05 sec/call)
 ** in fib ** spent time: 1.12 sec due to 33321 call(s) (3.364e-05 sec/call)
```

The algorithm for the distributed asynchron recursion is used by inheritance of `ctl::asynchron`, in the example also referred to as `baseT`. In order to minimise the number of remote invocations, already the constructor of the deriving class, here `fibonacci` starts and continues the recursion. In the case `n<2` this recursion stops. In order to yield asynchronous behaviour, the recursive calls `baseT::call` and `baseT::callLocal` do not wait for a result. In stead, a callback mechanism gives the result later back via the `operator()` together with its index to the calling `fibonacci`-instance. Each of these calls creates remotely (`baseT::call`) or locally (`baseT::callLocal`) a new `fibonacci`-instance which will be automatically destroyed, when it has received all results of all of its calls. Therefor, at this time the destructor `~fibonacci()` is invoked, which has to give the result `resM[0] + resM[1]` = fibonacci(n-1) + fibonacci(n-2) back to the algorithm by calling `baseT::set`.

The recursion is executed in parallel with automatic load balancing. This load balancing uses the book-holding information resulting from the termination control which is implemented by the vector method of Mattern [7]. The time measurement shows that the dominant working part of this algorithm i.e. the constructor of `fibonacci`, explains already dominantly the total runtime, see `ctl/examples3/recursion`.

References

[1] P. Birken, K. Quint, S. Hartmann, and A. Meister, *On coupling schemes for heat transfer in FSI applications*, Fluid-Structure-Interaction. Theory, Numerics and Applications (S. Hartmann, A. Meister, M. Schäfer, and S. Turek, eds.), Kassel University Press, 2009, pp. 21 – 30.

[2] P. Birken, K. Quint, S. Hartmann, and A. Meister, *Choosing norms in adaptive FSI calculations*, PAMM **10** (2010), no. 1, 555–556, doi:10.1002/pamm.201010270.

[3] J.-B. Colliat, M. Hautefeuille, and A. Ibrahimbegovic, *Meso- to macro-scale probability aspects for size effects and heterogenous materials failure*, pp. 253–275, ISTE, 2010, doi:10.1002/9780470611364.ch14.

[4] M. Krosche and M. Hautefeuille, *Simulation and solution of stochastic systems with a component-based software design*, PAMM **7** (2007), no. 1, 2140001–2140002, doi:10.1002/pamm.200700067.

[5] D. Markovic, R. Niekamp, A. Ibrahimbegović, H. G. Matthies, and R. L. Taylor, *Multi-scale modeling of heterogeneous structures with inelastic constitutive behaviour: Part i - physical and mathematical aspects*, Engineering Computations: Int J for Computer-Aided Engineering **22** (2005), no. 5-6, 664–683, doi:10.1108/02644400510603050.

[6] R. N. Markus Krosche and H. G. Matthies, *Platon: A problem solving environment for computational steering of evolutionary optimisation on the grid*, EUROGEN (G. Bugeda, J.A.-Désidéri, J. Periaux, M. Schoenauer, and G. Winter, eds.), 2003.

[7] F. Mattern, *Virtual time and global states of distributed systems*, Workshop on Parallel and Distributed Algorithms, Chateau de Bonas: France, Cosnard, M, Elsevier, 1988, pp. 215–226.

[8] H. G. Matthies, R. Niekamp, and J. Steindorf, *Algorithms for strong coupling procedures*, Computer Methods in Applied Mechanics and Engineering **195** (2006), no. 17 - 18, 2028 – 2049.

[9] R. Niekamp, D. Markovic, A. Ibrahimbegović, H. G. Matthies, and R. L. Taylor, *Multi-scale modelling of heterogeneous structures with inelastic constitutive behavior: Part ii - software coupling implementation aspects*, Engineering Computations: Int J for Computer-Aided Engineering **26** (2009), no. 1-2, 6–28, doi:10.1108/02644400910924780.

[10] J. Rang, M. Krosche, R. Niekamp, and H. G. Matthies, *Solving fluid-structure interaction problems using strong coupling algorithms with the component template library (ctl)*, PAMM **8** (2008), no. 1, 10987–10988, doi:10.1002/pamm.200810987.

[11] T. Srisupattarawanit, R. Niekamp, and H. G. Matthies, *Simulation of nonlinear random finite depth waves coupled with an elastic structure*, Computer Methods in Applied Mechanics and Engineering **195** (2006), no. 23 - 24, 3072 – 3086.

2.7 Stochastic Navier-Stokes equations are a coupled system

Ansprechpartner:	Joachim Rang
EMail:	j.rang@tu-bs.de
Telefon:	0531/391-3007

In this project the incompressible Navier–Stokes equations are considered with uncertainties, i.e. we assume that the Reynolds number, the boundary conditions and the right-hand side are not known exactly and modelled probabilistic. The numerical solution is determined with stochastic Galerkin methods and a low-rank approximation (see [2]). Therefore not only the input and the output quantities are represented. The aim of this project is to use this data format in the whole computing process.

Starting point of our considerations are the stationary incompressible Navier–Stokes equations which are given in dimensionaless form by

$$\begin{aligned} -\tfrac{1}{Re}\Delta u + (u\cdot\nabla)u + \nabla p &= f(t,x,\omega) && \text{in } \mathcal{G},\\ \nabla\cdot u &= 0 && \text{in } \mathcal{G}. \end{aligned} \tag{1}$$

Here, $x = (x_1, x_2, x_3)^\top \in \mathcal{G} \subseteq \mathbb{R}^3$, and ω is an elementary event of a realisation in a random space $(\Omega, \mathcal{A}, \mathbb{P})$ of random events. Moreover we need boundary and initial conditions for obtaining a unique solution of (1). Uncertain might be the right-hand side $f(t,x,\omega)$, the coefficients or the boundary conditions.

The stochastic solution $u(x,\omega)$ can be represented with the help of the isomorphies $L_2(\mathcal{G}\times\Omega) \cong L_2(\mathcal{G})\otimes L_2(\Omega)$ and $(\Omega,\mathcal{A},\mathbb{P}) \cong \Pi_{j=1}^{\infty}(\Omega_j,\mathcal{A}_j,\mathbb{P})$.

For the numerical approximation we need only finitely many random spaces $(\Omega_j,\mathcal{A}_j,\mathbb{P})$. For the representation of the solution not only the separation of deterministic and stochastic part are used. Moreover the solution is considered in a low-rank approximation where a further separation of the stochastic parts with the isomorphy

$$L_2\left(\mathcal{G}\times\prod_{j=1}^{M}\Omega_j\right) = L_2(\mathcal{G})\otimes\left(\bigotimes_{j=1}^{M} L_2(\Omega_j,\mathcal{A}_j,\mathbb{P})\right)$$

is used. A discretisation in the deterministic and in the stochastic domain with Finite Elements or Volumes and a stochastic Bubnov-Galerkin method lead to a nonlinear problem of the form

$$\mathbf{N}(\boldsymbol{v},\boldsymbol{v}) + \mathbf{K}\boldsymbol{v} + \mathbf{B}\boldsymbol{p} = \boldsymbol{g}, \text{ and } \mathbf{B}^T\boldsymbol{v} = 0.$$

The bilinear operator $\mathbf{N}(\cdot,\cdot)$ is obtained from the nonlinear convection, $\mathbf{K}$ is the matrix which belongs to the diffusive part, and $\mathbf{B}$ is the discretised gradient. Moreover $\boldsymbol{v}$ and $\boldsymbol{p}$ are vectors for the discrete velocity

v and for the discrete pressure p. If these terms are expanded in a PCE, i.e. with

$$\begin{aligned} \boldsymbol{v}(\theta(\omega)) &= \sum_{\alpha\in\mathcal{J}_M} \boldsymbol{v}^{(\alpha)} H_\alpha(\theta(\omega)), \quad \boldsymbol{p}(\theta(\omega)) = \sum_{\beta\in\mathcal{J}_M} \boldsymbol{p}^{(\beta)} H_\beta(\theta(\omega)), \\ \boldsymbol{g}(\theta(\omega)) &= \sum_{\gamma\in\mathcal{J}_M} \boldsymbol{g}^{(\gamma)} H_\gamma(\theta(\omega)), \end{aligned}$$

we obtain an explicite PCE representation of the nonlinear instationary incompressible Navier–Stokes equations, which can be written as

$$\begin{aligned} \mathbf{N}(\boldsymbol{v},\boldsymbol{v}) + (\mathbf{K}\otimes matI)\boldsymbol{v} + (\mathbf{B}\otimes\mathbf{I})\boldsymbol{p} &= \boldsymbol{g}, \\ \text{and } (\mathbf{I}\otimes\mathbf{B}^T)\boldsymbol{v} &= 0. \end{aligned}$$

This is a coupled system of nonlinear equations (see [3] for more details). Therefore the stochastic quantities may be represented in a low-rank format to reduce the dimension of the system.

The numerical solution of this system can be computed with a partitioned solution strategy, i.e. each subsystem is solved separatedly from each other. Often the so-called Block-Jacobi method is applied. This method can be easily parallelised and a convergence proof can be found in [1].

Literatur

[1] L. Giraldi, A. Litvinenko, H. G. Matthies, and A. Nouy, *To be or not be intrusive? The solution of parametric and stochastic equations - the "plain vanilla" Galerkin case*, arxiv:1309.1617, 2013.

[2] H. G. Matthies, *Uncertainty quantification with stochastic finite elements*, Encyclopedia of Computational Mechanics (E. Stein, R. de Borst, and T. R. J. Hughes, eds.), John Wiley & Sons, Chichester, 2007.

[3] J. Rang and H. G. Matthies, *Stochastic Navier-Stokes equations are a coupled system*, Computational Methods in Marine Engineering V, Proceedings Marine 2013, Hamburg (B. B. und P. Wriggers, ed.), CIMNE, Barcelona, 2013, pp. 278–288, URL: congress.cimne.com/marine2013/frontal/doc/Ebook%20-%20Marine%202013.pdf.

2.8 An analysis of the Prothero-Robinson example for constructing new Rosenbrock–Wanner methods

Ansprechpartner:	Joachim Rang
EMail:	j.rang@tu-bs.de
Telefon:	0531/391-3007

2.8.1 Introduction

One possibility to solve stiff ODEs like the example of Prothero and Robinson [4] or differential algebraic equations are corresponding Runge-Kutta methods [1, 8]. The theoretical convergence order may not be achieved [1, 8], in this case, i.e. the so-called order reduction phenomenom can be observed. In the last years many papers were published considering this phenomenom [6].

In this project diagonally implicit Runge–Kutta methods (DIRK methods) and Rosenbrock–Wanner methods (ROW methods) are applied on the example of Prothero and Robinson. Then the local and the global error are computed. It can be shown that DIRK or ROW methods should satisfy some further order conditions to avoid order reduction.

2.8.2 New order conditions

Consider an ODE of the form $\dot{\boldsymbol{u}} = \boldsymbol{F}(t, \boldsymbol{u})$ with the initial condition $\boldsymbol{u}(0) = \boldsymbol{u}_0$. A Rosenbrock–Wanner–method (ROW–method) with s internal stages is given by the formulas

$$\boldsymbol{k}_i = \boldsymbol{F}\left(t_m + \alpha_i \tau_m, \tilde{\boldsymbol{U}}_i\right) + \tau_m J \sum_{j=1}^{i} \gamma_{ij} \boldsymbol{k}_j + \tau_m \gamma_i \dot{\boldsymbol{F}}(t_m, \boldsymbol{u}_m), \tag{2}$$

$$\tilde{\boldsymbol{U}}_i = \boldsymbol{u}_m + \tau_m \sum_{j=1}^{i-1} \alpha_{ij} \boldsymbol{k}_j, \quad i = 1, \ldots, s,$$

$$\boldsymbol{u}_{m+1} = \boldsymbol{u}_m + \tau_m \sum_{i=1}^{s} b_i \boldsymbol{k}_i, \tag{3}$$

where $J := \partial_{\boldsymbol{u}} \boldsymbol{F}(t_m, \boldsymbol{u}_m)$, α_{ij}, γ_{ij}, b_i are the parameters of the method, and

$$\alpha_i := \sum_{j=1}^{i-1} \alpha_{ij}, \quad \gamma_i := \sum_{j=1}^{i-1} \gamma_{ij}, \quad \gamma := \gamma_{ii} > 0, \ i = 1, \ldots, s.$$

If we apply the ROW method to the example of Prothero and Robinson and use a Taylor expansion we get a representation of the local error

$$\begin{aligned}\delta_\tau(t_{m+1}) = &\sum_{k=2}^{p-1}\left[\boldsymbol{b}^\top\mathbf{B}^{-1}\boldsymbol{\alpha}^k - 1\right]\varphi_m^{(k)}\frac{\tau^k}{k!} + \mathcal{O}(\tau^{p+1})\\ &+\sum_{k=2}^{p+1}\boldsymbol{b}^\top\sum_{l=1}^{k-2}\left\{\mathbf{B}^{-l-1}\left[\boldsymbol{\alpha}^{k-l}+\boldsymbol{\gamma}\delta_{k-l,1}\right]\frac{1}{(k-l)}\right.\\ &\left.-\mathbf{B}^{-l}\left[\alpha^{k-l-1}+\gamma\delta_{k-l-1,1}\right]\right\}\cdot\varphi_m^{(k-l)}\frac{\tau^{k-l}}{(k-l-1)!z^l},\end{aligned}$$

where $\mathbf{B} = (\beta_{ij})_{i,j=1}^s$, $\boldsymbol{b} = (b_1,\ldots,b_s)^\top$, $\boldsymbol{\alpha} = (\alpha_1,\ldots,\alpha_s)^\top$, and $\gamma = (\gamma_1,\ldots,\gamma_s)^\top$. Finally we get the new order conditions (see [6] for more informations)

$$\boldsymbol{b}^\top\mathbf{B}^{-1}\boldsymbol{\alpha}^k = 1, \quad k = 2,\ldots,p, \tag{4}$$

$$\boldsymbol{b}^\top\mathbf{B}^{-(l+1)}\frac{1}{k-l}\boldsymbol{\alpha}^{k-l} = \boldsymbol{b}^\top\mathbf{B}^{-l}\left[\boldsymbol{\alpha}^{k-l-1}+\gamma\delta_{k-l-1,1}\right], \tag{5}$$

for $l = 1,\ldots,k-2$ and $k = 1,\ldots,p+1$. Note that order conditions derived by Lubich and Ostermann in [3] are special cases of our new order conditions. A similar calculation can be done for the DIRK–methods (see [6]). In this case we obtain

$$\boldsymbol{b}^\top\mathbf{A}^{-1}\boldsymbol{c}^k = 1, \quad k = 2,\ldots,p, \tag{6}$$

$$\boldsymbol{b}^\top\mathbf{A}^{-(l+1)}\frac{1}{k-l}\boldsymbol{c}^{k-l} = \boldsymbol{b}^\top\mathbf{A}^{-l}\boldsymbol{c}^{k-l-1}, \tag{7}$$

for $l = 1,\ldots,k-2$ and $k = 1,\ldots,p+1$. Conditions (4) and (6) are automatically satisfied if the method is stiffly accurate. In [5] the method ROS34PW2 is equipped with the new order conditions and in [7] traditional ROW-method like ROS3P, ROS3PL and RODASPRL are modified in such a way that they met the new order conditions.

2.8.3 Numerical results

Let J be a time interval and $\Omega \subset \mathbb{R}^d$ be a domain. We consider the incompressible Navier–Stokes equations which are given in dimensionless form by

$$\begin{aligned}\dot{u} - Re^{-1}\Delta u + (u\cdot\nabla)u + \nabla p &= f \quad \text{in } J\times\Omega,\\ \nabla\cdot u &= 0 \quad \text{in } J\times\Omega,\\ u &= g \quad \text{on } J\times\partial\Omega,\\ u(0,x) &= u_0 \quad x\in\Omega,\end{aligned} \tag{8}$$

where Re denotes the positive Reynolds number. Details to the discretisation in space and time can be found for example in [2] and the references cited in there. In our first example of the incompressible

Navier–Stokes equations the right-hand side f, the initial condition u_0 and the non-homogeneous Dirichlet boundary conditions are chosen such that

$$\begin{aligned} u_1(t,x,y) &= \sin(t)(y^2+x), \\ u_2(t,x,y) &= \sin(t)(x^2-y), \\ p(t,x,y) &= \exp(-t)(x+y-1) \end{aligned}$$

is the exact solution of (8). Moreover we set $Re = 1$, $\Omega = (0,1)^2$ and solve the problem in the time interval $(0, 1/10]$. We use the Q_2/P_1^{disc} discretisation on a uniform mesh which consists of squares with an edge length $h = 1/32$. Note that for any t the solution can be represented exactly by discrete functions. Hence, all occurring errors will result from the temporal discretisation. During the calculations we have to deal with 8,450 d.o.f. for the velocity and 3,072 d.o.f. for the pressure. As time steps we use $\tau = \frac{1}{10 \cdot 2^k}$, $k = 0, \ldots, 7$. The numerical results are presented

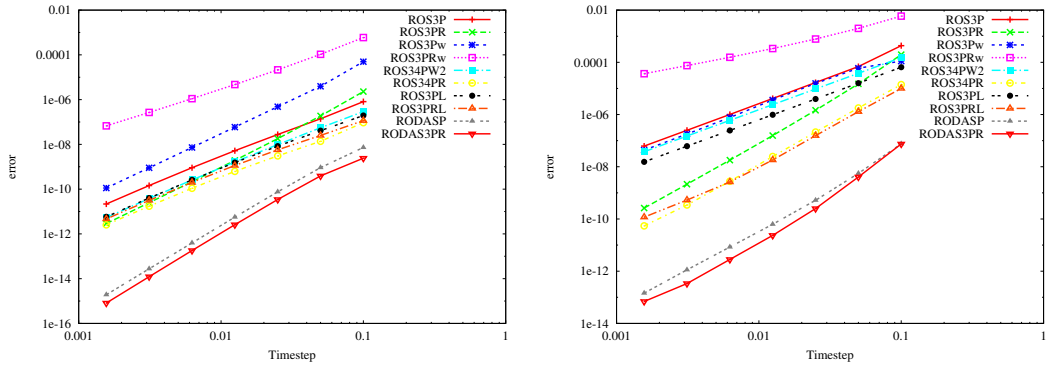

Figure 18: τ versus error for (8) velocity u (left) and pressure p (right)

in Figure 18. Considering the velocity error it can be observed that all chosen schemes converge with order 3 or 4 as expected. In the case of the pressure component it can be observed that the new methods provide more accurate results than the older ones, since the older methods do not satisfy the new order conditions from [6].

References

[1] E. Hairer and G. Wanner, *Solving ordinary differential equations. II: Stiff and differential-algebraic problems*, Springer Series in Computational Mathematics, vol. 14, Springer-Verlag, Berlin, 1996.

[2] V. John and J. Rang, *Adaptive time step control for the incompressible Navier–Stokes equations*, Comput. Methods Appl. Mech. Eng. **199** (2010), 514–524.

[3] C. Lubich and A. Ostermann, *Linearly implicit time discretization of non-linear parabolic equations.*, IMA J. Numer. Anal. **15** (1995), no. 4, 555–583.

[4] A. Prothero and A. Robinson, *On the stability and accuracy of one-step methods for solving stiff systems of ordinary differential equations*, Math. Comp. **28** (1974), 145–162.

[5] J. Rang, *A New Stiffly Accurate Rosenbrock-Wanner Method for Solving the Incompressible Navier-Stokes Equations*, Recent Developments in the Numerics of Nonlinear Hyperbolic Conservation Laws (R. Ansorge, H. Bijl, A. Meister, and T. Sonar, eds.), vol. 120, Springer Verlag, Heidelberg, Berlin, 2012, pp. 301–315.

[6] J. Rang, *An analysis of the Prothero-Robinson example for constructing new DIRK and ROW methods*, Journal of Computational and Applied Mathematics (2013), doi:http://dx.doi.org/10.1016/j.cam.2013.09.062.

[7] J. Rang, *Improved traditional Rosenbrock–Wanner methods for stiff ODEs and DAEs*, Informatik-Bericht 2013-05, TU Braunschweig, Braunschweig, 2013, URL: http://www.digibib.tu-bs.de/?docid=00055262.

[8] K. Strehmel and R. Weiner, *Linear-implizite Runge–Kutta-Methoden und ihre Anwendung*, Teubner-Texte zur Mathematik, vol. 127, Teubner, Stuttgart, 1992.

2.9 Adaptive timestep control for the generalised-α method

Ansprechpartner:	Joachim Rang
EMail:	j.rang@tu-bs.de
Telefon:	0531/391-3007

2.9.1 Introduction

The generalised-α methods are usually of second order and allow the damping of high frequencies, which can be controlled by certain parameters. Second order accuracy can be achieved if a further order condition is satisfied. Together with stability conditions (see [2]) a robust and effective class of methods is obtained.

For solving ODEs or DAEs a good time integration method needs an error estimator to increase efficiency. This error estimator suggests a new timestep size to reach a given accuracy. If the timestep size is too small much unnecessary computational work has to be done. Otherwise, if the timestep size is too large, the results become less accurate.

2.9.2 The generalised-α method for 1st order ODEs

In the following we consider the ODE

$$\dot{\boldsymbol{u}} = \boldsymbol{f}(t, \boldsymbol{u}), \quad \boldsymbol{u}(0) = \boldsymbol{u}_0. \tag{9}$$

To determine the numerical solution of (9) we use the generalised-α method, which is given by the formulas

$$\dot{\boldsymbol{u}}_{n+\alpha_m} = \boldsymbol{f}(t_{n+\alpha_f}, \boldsymbol{u}_{n+\alpha_f}), \tag{10}$$
$$\boldsymbol{u}_{n+1} = \boldsymbol{u}_n + \tau\dot{\boldsymbol{u}}_n + \tau\gamma(\dot{\boldsymbol{u}}_{n+1} - \dot{\boldsymbol{u}}_n), \tag{11}$$
$$\dot{\boldsymbol{u}}_{n+\alpha_m} = \dot{\boldsymbol{u}}_n + \alpha_m(\dot{\boldsymbol{u}}_{n+1} - \dot{\boldsymbol{u}}_n), \tag{12}$$
$$\boldsymbol{u}_{n+\alpha_f} = \boldsymbol{u}_n + \alpha_f(\boldsymbol{u}_{n+1} - \boldsymbol{u}_n). \tag{13}$$

It is well known that the generalised-α method can be formulated as a one-step and a two-step method. First we manipulate the formulas (10)–(13) to obtain a non-linear system consisting of two decoupled equations. For simplification we define $\boldsymbol{f}_{n+\alpha_f} := \boldsymbol{f}(t_{n+\alpha_f}, \boldsymbol{u}_{n+\alpha_f})$. A simple calculation gives

$$\boldsymbol{u}_{n+1} = \boldsymbol{u}_n + \tau\left(1 - \frac{\gamma}{\alpha_m}\right)\dot{\boldsymbol{u}}_n + \frac{\tau\gamma}{\alpha_m}\boldsymbol{f}_{n+\alpha_f}, \tag{14}$$
$$\dot{\boldsymbol{u}}_{n+1} = \frac{1}{\tau\gamma}\left(\boldsymbol{u}_{n+1} - \boldsymbol{u}_n - \tau(1-\gamma)\dot{\boldsymbol{u}}_n\right), \tag{15}$$

if $\alpha_m \neq 0$. The starting value $\dot{\boldsymbol{u}}_0$ can be computed from the ODE (9).

2.9.3 Adaptivity

If the generalised-α methods are formulated as onestep methods the so-called PI-controller from Gustafsson et. al. [3] can be used. To suggest a new timestep size we need a second solution of order 1, in our case we use the backward Euler method. The next timestep size τ_{n+1} is proposed to be

$$\tau_{n+1} = \rho \frac{\tau_n^2}{\tau_{n-1}} \left(\frac{TOL \cdot r_n}{r_{n+1}^2} \right)^{1/2}, \tag{16}$$

where $\rho \in (0, 1]$ is a safety factor, $TOL > 0$ is a given tolerance, and $r_{n+1} := \|\boldsymbol{u}_{n+1} - \hat{\boldsymbol{u}}_{n+1}\|$. In [1, 8] different error measures can be found, which use a combination of relative and absolute errors. For further details about the numerical error and the implementation of automatic steplength control we refer to [1]. The algorithm reads as follows:

- Compute the numerical solution $(\boldsymbol{u}_{n+1}, \dot{\boldsymbol{u}}_{n+1})^\top$ with the help of the generalised-α method (14), (15).
- Compute the second solution with the backward Euler method and use $\dot{\boldsymbol{u}}_{n+1}$ as approximation for $\boldsymbol{f}(t_{n+1}, \boldsymbol{u}_{n+1})$, i.e. $\hat{\boldsymbol{u}}_{n+1} = \boldsymbol{u}_n + \tau_n \dot{\boldsymbol{u}}_{n+1}$.
- Compute the numerical error with r_{n+1} and approximate the new timestep length τ_{n+1} with (16).
- If the numerical error is smaller than the given tolerance the timestep is accepted, otherwise it is rejected and has to be recomputed with the new timestep length τ_{n+1}.

This chemical reaction problem is called E5 and can be found in the collection by Enright, Hull, and Lindberg [1]. The equations are given by

$$\begin{aligned}
\dot{u}_1 &= -Au_1 - Bu_1u_3, \\
\dot{u}_2 &= Au_1 - MCu_2u_3, \\
\dot{u}_3 &= Au_1 - Bu_1u_3 - MCu_2u_3 + Cu_4, \\
\dot{u}_4 &= Bu_1u_3 - Cu_4
\end{aligned}$$

with the initial conditions $u_1(0) = 1,76 \times 10^{-3}$ and $u_i(0) = 0$, $i \in \{2, 3, 4\}$. Moreover we set as in [1] $A = 7,89 \times 10^{-10}$, $B = 1,1 \times 10^7$, $C = 1,13 \times 10^3$, and $M = 10^6$. The equations should be solved in the time interval $[0, 10^{13}]$. Note that the variables u_2, u_3, and u_4 satisfy the equation $u_2 - u_3 - u_4 = 0$. The parameter ρ is chosen to be 0, 1/4, 1/2, 3/4, and 9/10, resp. For ρ tending to 1 the algorithm becomes instable. We compare the generalised-α methods with other implicit and linear-implicit second order solvers like ROS2, ROS2S and the method

of Ellsiepen. It can be observed from Figure 19 that the generalised-α methods with the new stepsize controller are more effective than the other second order methods. An adaptive algorithm for second order

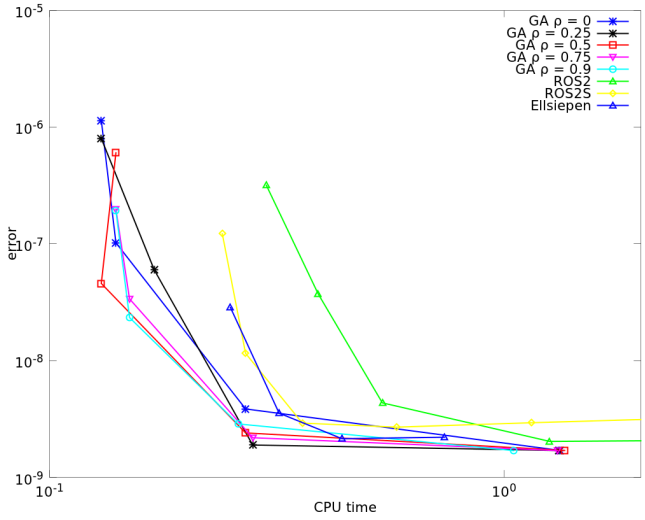

Figure 19: Comparison of generalised-α methods for first order ODEs: CPU time versus error

problem can be realised in an analogous way (see [4]).

References

[1] W. Enright, T. Hull, and B. Lindberg, *Comparing numerical methods for stiff systems of O.D.E:s.*, BIT, Nord. Tidskr. Inf.-behandl. **15** (1975), 10–48 (English), doi:10.1007/BF01932994.

[2] S. Erlicher, L. Bonaventura, and O. S. Bursi, *The analysis of the generalized-α method for non-linear dynamic problems*, Comput. Mech. **28** (2002), no. 2, 83–104.

[3] K. Gustafsson, M. Lundh, and G. Söderlind, *A PI stepsize control for the numerical solution of ordinary differential equations.*, BIT **28** (1988), no. 2, 270–287.

[4] J. Rang, *Adaptive timestep control for the generalised-α method*, Adaptive Modelling and Simulation (D. Aubry, P. Diez, B. Tie, and N. Paréz, eds.), CIMNE, Barcelona, 2013, pp. 559–570, URL: http://congress.cimne.com/coupled2013/frontal/doc/Coupled13_ebook.pdf.

2.10 Apdative timestep control for fully implicit Runge–Kutta methods of higher order

Ansprechpartner:	Joachim Rang
EMail:	j.rang@tu-bs.de
Telefon:	0531/391-3007

2.10.1 Introduction

An adaptive time step control may undoubtedly improve the accuracy and efficiency of simulations substantially. One possibility to achieve adaptivity in time is Richardson's extrapolation. A much cheaper possibility is the so-called embedding technique where the second solution is computed with almost the same coefficients, such that no further costs for linear algebra arise [4, 8]. In practice this technique is only applied if the order of both methods differ by only one. Therefore Hairer and Wanner suggest in [5] a new step size control for Raudau-methods where an automatic choice of Radau methods of different order is integrated. An improvement for a Radau-IIA method of order 17 can be found in [6].

In this project fully implicit Runge–Kutta (FIRK) methods of higher order are equipped with an embedded method such that an adaptive time step control is possible. The embedded FIRK method has order $s-1$, where s is the number of internal stages.

The disadvantage of this class of methods is the cost for the linear algebra. In every time step a non-linear system of dimension ns has to be solved, where n is the dimension of the problem and s is the number of internal stages of the Runge–Kutta method. In [2] and [1] a transformation of the coefficient matrix of the Runge–Kutta method is introduced. If a simplified Newton method is applied this splitting leads to s (may be complex valued) systems of dimension n. An application of this technique for Radau methods can be found in [5]. These non-linear systems can be solved directly with the help of LU-decompositions and back- and forward substitutions. In the case of the simplified Newton methods for higher order methods a stepsize restriction can be observed (see [7]). With the results from Deuflhard [3] the largest possible stepsize can be estimated. Since this stepsize is rather small in [7] other nonlinear solvers like the modified fixedpoint iteration are considered.

2.10.2 Implicit Runge–Kutta methods

We start our considerations with the initial value problem

$$\dot{\boldsymbol{u}} = \boldsymbol{f}(t, \boldsymbol{u}), \quad \boldsymbol{u}(t_0) = \boldsymbol{u}_0. \tag{17}$$

A FIRK method for the ODE (17) is given by

$$\boldsymbol{k}_i = \boldsymbol{f}\left(t_m + c_i\tau, \boldsymbol{u}_m + \tau_m \sum_{j=1}^{s} a_{ij}\boldsymbol{k}_j\right), \quad i = 1, \ldots, s, \tag{18}$$

$$\boldsymbol{u}_{m+1} = \boldsymbol{u}_m + \tau_m \sum_{i=1}^{s} b_i \boldsymbol{k}_i, \tag{19}$$

where τ is a given time step size, s is the number of internal stages and a_{ij}, b_i, and c_i are the coefficients of the RK-method, which should be determined in such a way that the method has a sufficiently high order convergence [4, 8]. The order of the RK-method can be determined with the so-called simplifying conditions from Butcher, which are given by

$$\begin{aligned}
B(p): &\quad \sum_{i=1}^{s} b_i c_i^{k-1} &&= 1/k, && k = 1, \ldots, p,\\
C(q): &\quad \sum_{j=1}^{s} a_{ij} c_j^{k-1} &&= c_i^k/k, && i = 1, \ldots, s, k = 1, \ldots, q,\\
D(r): &\quad \sum_{i=1}^{s} b_i c_i^{k-1} a_{ij} &&= b_j(1 - c_j^k)/k, && j = 1, \ldots, s, k = 1, \ldots, r.
\end{aligned}$$

The condition $B(p)$ is equivalent to a quadrature rule with nodes c_i and weights b_i, which integrates polynomials of degree $p-1$ exactly. The conditions $C(q)$ have the following meaning. The intermediate values $\boldsymbol{k}_i$ are integrated exactly by a quadrature rule with weights a_{ij} and nodes c_i, which integrates polynomials of degree q exactly.

FIRK methods can be derived with the roots of the shifted Legendre polynomial of degree s. These roots are then chosen as nodes c_i in the FIRK method. With the simplifying conditions $B(p)$ the weights b_i are uniquely determined and the coefficients a_{ij} are computed and with the conditions $C(s)$ or $D(r)$, depending on the method (see [4, 8, 7]). In the case of the Gauß quadrature rules the condition for the embedded method reads as

$$\vec{\tilde{e}}_H^{\top} := \left(1, \frac{1}{2}, \ldots, \frac{1}{s-1}, 0\right).$$

Then the nodes $\tilde{b}_i$ are given simply by $\vec{\tilde{b}}^{\top} = \vec{\tilde{e}}_H^{\top} V_s^{-1}$ and the embedded method is of order $s-1$. The Butcher table is then given by

$$\begin{array}{c|c} \boldsymbol{c} & \mathbf{C}\mathbf{V}_s^{-1} \\ \hline & \boldsymbol{e}_H^{\top}\mathbf{V}_s^{-1} \\ \hline & \tilde{\boldsymbol{e}}_H^{\top}\mathbf{V}_s^{-1} \end{array}.$$

Other classes of FIRK methods are considered in [7].

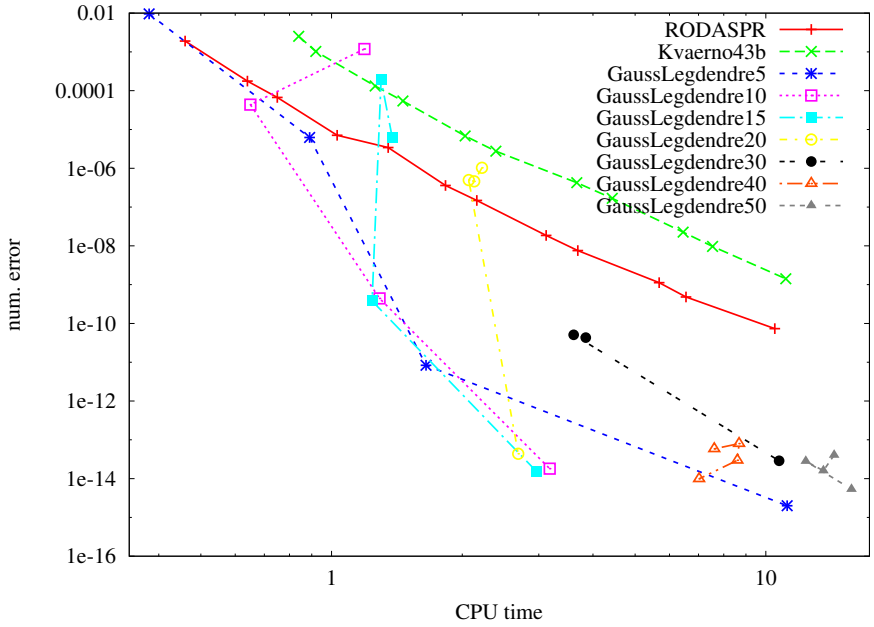

Figure 20: Numerical results

2.10.3 Numerical examples for ODEs

Consider the second order ODE

$$\ddot{y}_i = -\frac{y_i}{(y_1^2+y_2^2)^{3/2}} - \epsilon\frac{3y_i}{2(y_1^2+y_2^2)^{5/2}}, \quad i=1,2,$$

where ϵ is a small perturbation. If $\epsilon = 0$ we get the original Kepler problem. The initial conditions are given by

$$y_1 = 0, \quad y_2 = \sqrt{\frac{1+e}{1-e}}, \quad \dot{y}_1 = 1-e, \quad \dot{y}_2 = 0,$$

where $e \in [0,1)$ is a parameter. We solve this problem in the time interval $(0, 1000]$ and we measure as numerical error the Hamiltonian function. The numerical results are shown in Figure 20. It can be observed that the numerical error tends to 1.0E-16 for all methods. The most efficient methods are with 10 and 15 internal stages. For methods with more than 15 internal stages the dimension of the non-linear systems is too large, and the step size restriction plays an important role. Therefore this methods are not so efficient. The RODASPR method and the Kvaerno43b method are the most inefficient since they are only of order 4 and need too many time steps. For more examples and methods we refer to [7].

2.10.4 Outlook

Since the solutions of the huge non-linear systems are very expensive, the costs can be reduced by splitting these systems into s smaller ones. One possibility is a transformation of coefficient matrix A, which was

derived independently from Bickart [1] and Butcher [2]. Then we systems can be solved in parallel with the help of the Component Template Library (CTL). One application can be the incompressible Navier-Stokes equations since high dimensional systems have to be solved and the convergence order of pressure can be higher as in the case of other onestep methods.

References

[1] T. A. Bickart, *An efficient solution process for implicit Runge-Kutta methods.*, SIAM J. Numer. Anal. **14** (1977), 1022–1027 (English), doi:10.1137/0714069.

[2] J. Butcher, *On the implementation of implicit Runge-Kutta methods.*, BIT **16** (1976), 237–240 (English), doi:10.1007/BF01932265.

[3] P. Deuflhard, *Newton methods for nonlinear problems. Affine invariance and adaptive algorithms.*, Springer-Verlag, Berlin, 2004 (English).

[4] E. Hairer and G. Wanner, *Solving ordinary differential equations. II: Stiff and differential-algebraic problems*, Springer Series in Computational Mathematics, vol. 14, Springer-Verlag, Berlin, 1996.

[5] E. Hairer and G. Wanner, *Stiff differential equations solved by Radau methods.*, J. Comput. Appl. Math. **111** (1999), no. 1-2, 93–111 (English), doi:10.1016/S0377-0427(99)00134-X.

[6] J. Martín-Vaquero, *A 17th-order radau IIA method for package* `RADAU`. *Applications in mechanical systems.*, Comput. Math. Appl. **59** (2010), no. 8, 2464–2472 (English), doi:10.1016/j.camwa.2009.12.025.

[7] J. Rang, *Apdative timestep control for fully implicit Runge–Kutta methods of higher order*, Informatik-Bericht 2014-03, TU Braunschweig, Braunschweig, 2014, URL: http://www.digibib.tu-bs.de/?docid=00055783.

[8] K. Strehmel and R. Weiner, *Linear-implizite Runge–Kutta-Methoden und ihre Anwendung*, Teubner-Texte zur Mathematik, vol. 127, Teubner, Stuttgart, 1992.

2.11 Computational approaches to Bayesian updating

Ansprechpartner:	Bojana Rosić
EMail:	bojana.rosic@tu-bs.de
Telefon:	0531/391-3016

The investigation of the uncertainty updating methods is done in the framework of two projects QUANTIMAT (Deutsche Forschungsgemeinschaft project) and SOMUPAK (Deutscher Akademischer Austauschdienst travel project), realised in cooperation with the Technical University in Prague and University of Kragujevac, respectively. These projects are focusing on the uncertainty quantification and updating in the description of heterogeneous materials. The goal is to develop computationally fast and reliable Bayesian updating procedures.

Estimation of material properties from noisy experimental measurements can be approached in different ways, either in form of proper deterministic regularisation procedure [1] or via probabilistic Bayesian inference [9]. Most of deterministic-like studies are approaching the problem by considering the observed and predicted system responses and tunning the parameters such that the distance between those two is minimised. However, the consequent optimisation problem is often ill-posed - the minimised function is multimodal, non-smooth or non-differentiable - and hence one of the regularisation procedures [1] is required. Such a fitting-based approach provides only one point estimate and omits the related uncertainties in measurements, imperfections of the numerical model as well as the preliminary knowledge about the material parameters arising from their physical occurrence.

In a probabilistic—Bayesian—point of view the unknown parameters are taken to be uncertain and modelled with the help of the random variables/fields (RVs) whose probability descriptions are obtained from the experts knowledge and the maximum entropy law [9, 5]. In this regard, the process of obtaining more information through experiments becomes well-posed. Unlike the point-estimate techniques, this concept transforms the prior expert-based probability description to the posterior with the help of given data and the Bayes' theorem. As a final outcome, the posterior distribution summarizes all available information about the model parameters such as the mean value, variance, probability of occurrence etc.

The primary computational challenge in Bayesian inference consist in extracting information from the posterior. Most of existing computational procedures take the form of particle filters which update the probability measure via sampling. A typical example is the Markov chain Monte Carlo (MCMC) method ([2]). The MCMC is known to be a very

general procedure which does not require any model approximations. The method constructs a Markov chain with an equilibrium distribution which corresponds to the posterior or conditional distribution. Its advantage is that it does not need target probabilities but only ratios of target probabilities to work. However, the method converges slowly according to the law of large numbers (Theorem 3 in [10]). The convergence is assured regardless of the starting point, however the speed of the convergence greatly depends on it. For each evaluation the method requires the approximate solution of a partial differential equation, i.e. the solution of the stochastic forward problem. Therefore, MCMC is known to be computationally expensive when used in practical applications.

In order to overcome this issue, we recently developed much faster but still reliable updating procedure by replacing the computationally expensive forward simulation with the surrogate solution in a form of a polynomial chaos expansion (PCE), see [3, 7]. Such an approximation leads to a significant reduction of the computation time as the evaluation of the PCE is cheap. However, one may show that this reduction is not enough if the method is supposed to be used in real-time systems. This is caused by the slow convergence of the MCMC method, which often requires more than 10^6 samples to approach a stationary posterior distribution. Due to those previously mentioned reasons, another fast and reliable computational procedure [7, 6, 8] has been built. The method updates the random variable by transforming its prior functional approximation (i.e. PCE) into the posterior one with the help of polynomial approximation of measurements. This is a completely different procedure from the previously mentioned, as the update of the probability measure is substituted with the random variable update. The estimator is of a minimum-variance type and represents a generalisation of Gauss-Markov theorem [4].

The numerical comparison of the developed procedures is investigated on the example of the linear diffusion equation, where the value of the diffusion coefficient is estimated with the help of noisy measurements of the temperature field. The true value of the thermal conductivity is taken to be one realisation of a lognormal random variable described independently from the a priori distribution—the so called truth. The corresponding data set—observations–are then obtained with the help of the deterministic finite-difference (FD) approach. Each measurement is subjected to Gaussian noise with zero mean and covariance matrix $C_\varepsilon = \sigma_\varepsilon^2 I$ (I is the identity matrix). As depicted in Fig. 21, the "virtual truth" is taken to lie in

- C1: high probability ($\kappa_t = 2$),
- C2: 2σ ($\kappa_t = 1.7$),

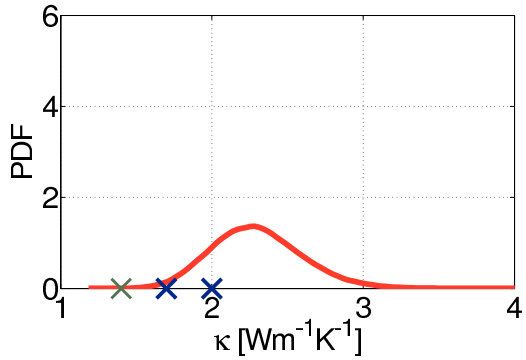

Figure 21: The description of the real data in three case scenarios

- and C3: low probability ($\kappa_t = 1.4$)

regions of the prior. While the first case scenario C1 represents the reliable assumption of the prior, the other two case scenarios are describing the situations in which one cannot have precise expert knowledge on the value of the parameter κ.

Method	Mode			Std		
	C1	C2	C3	C1	C2	C3
Truth	2	1.7	1.4	0	0	0
MCMC	1.9979	1.6952	1.4102	0.0131	0.0123	0.0163
LBUone	2.0016	1.6404	1.2345	0.0117	0.0096	0.0072
LBUall	2.0017	1.6404	1.2345	0.0184	0.0151	0.0113
SQRT	2.0018	1.6405	1.2346	0.0274	0.0225	0.0169
EnKF	2.0023	1.6441	1.2247	0.0262	0.0202	0.0158
EnKFSQRT	2.0026	1.6443	1.2250	0.0262	0.0207	0.0160

Table 2: The comparison of the posterior mean values and standard deviations for different update procedures in case of nonlinear measurement

The update process is performed only once using the complete measurement data. For comparison purposes, several computational strategies are applied: one random variable based linear Bayesian update (LIBone), full linear Bayesian update (LIBall), the square root update (SQRT), Ensemble Kalman filter (EnkF) with 1000 samples, square root Ensemble Kalman filter (EnkFSQRT) with 1000 samples and the full Bayesian MCMC update with 10^5 samples. The results obtained, as shown in Tab. 2, indicate that the MCMC procedure is the only one which can identify the truth in all three case scenarios. In contrast to this, the linear approximants are able to estimate the truth only in the first case scenario although with an overestimated standard deviation. The overestimation appears to be stronger in case of the square root posterior, as well as posteriors obtained from the ensemble data (EnKF-kind of procedures). Since the square root estimation is not equivalent to the linear Bayesian and since the ensemble Kalman filter estimates are strongly dependent on the chosen seed (here 1000 samples), this finding

was expected. Contrary to expectations, the one random variable linear Bayesian update is underestimating the posterior variance. It seems that the underestimation happens due to constraints put on the basis on which the posterior is projected. Namely, the one random variable linear Bayesian update is neglecting (projecting out) the additional random variables coming from the measurement data in the process of updating.

To get an adequate understanding of the conclusions drawn previously, we considered also the experiments in which the measurement operator is "more" linear, i.e. the temperature is inverted and log-transformed. Note that the nonlinear transformation is applied on the measurement data solely, i.e. without the measurement error. The measurement error is assumed to be Gaussian and in the same percentage value as in the nonlinear case.

Methods	Mode			Std		
	C1	C2	C3	C1	C2	C3
Truth	2	1.7	1.4	0	0	0
MCMC	1.9982	1.7109	1.4878	0.0342	0.0269	0.0209
LBUone	2.0020	1.7044	1.4062	0.0054	0.0039	0.0034
LBUall	2.0023	1.7046	1.4064	0.0332	0.0281	0.0232
SQRT	2.0023	1.7046	1.4064	0.0339	0.0288	0.0241
EnKF	2.0024	1.7038	1.4046	0.0340	0.0294	0.0237
EnKFSQRT	2.0022	1.7043	1.4054	0.0339	0.0290	0.0245

Table 3: The comparison of the posterior mean values and standard deviations for different update procedures

This study produced results which confirm the findings of a great deal of previous work in this field, see [7, 6, 8]. Namely, as results in Tab. 3 show, the methods based on the linear Bayesian formula are able to identify the truth in all three case scenarios without strong overestimations of variance. However, this is not the case for the one random variable based linear Bayesian update. This method underestimates the posterior variance similarly to the case study already discussed prevously. Therefore, the use of the one random variable based linear Bayesian update is not advised in practice. Furthermore, the MCMC procedure shows slightly different behaviour than in the nonlinear case. The nonlinear transformation of the predicted measurement and observation data in a polynomial chaos form has resulted in poor posterior estimation in the worst case scenario when the truth takes value in the low probability region of the prior. The problem appears due to large numerical errors caused by both sampling and transformation.

Acknowledgments: The author would like to thank to Dr. Anna Kučerová and Dr. Jan Sýkora from Technical University Prague on the QUANTIMAT project cooperation, as well as to the Department of

Computational Mechanics, University of Kragujevac on the SOMUPAK project cooperation.

References

[1] H. W. Engl, M. Hanke, and A. Neubauer, *Regularization of inverse problems*, Dordrecht: Kluwer, 2000.

[2] D. Gamerman and H. F. Lopes, *Markov Chain Monte Carlo: Stochastic simulation for bayesian inference*, Chapman and Hall/CRC, 2006.

[3] A. Kučerová, J. Sýkora, B. Rosić, and H. G. Matthies, *Acceleration of uncertainty updating in the description of transport processes in heterogeneous materials*, Journal of Computational and Applied Mathematics **236** (2012), no. 18, 4862–4872, doi:10.1016/j.cam.2012.02.003.

[4] D. G. Luenberger, *Optimization by vector space methods*, John Wiley & Sons, New York, London, Sydney, Toronto, 1969.

[5] Y. M. Marzouk, H. N. Najm, and L. A. Rahn, *Stochastic spectral methods for efficient Bayesian solution of inverse problems*, Journal of Computational Physics **224** (2007), no. 2, 560–586.

[6] O. Pajonk, B. Rosić, A. Litvinenko, and H. G. Matthies, *A deterministic filter for non-Gaussian Bayesian estimation*, Physica D: Nonlinear Phenomena **241** (2012), no. 7, 775–788, doi:10.1016/j.physd.2012.01.001.

[7] B. Rosić, A. Kučerová, J. Sýkora, O. Pajonk, A. Litvinenko, and H. G. Matthies, *Parameter identification in a probabilistic setting*, Engineering Structures, availible online (2013), doi:10.1016/j.engstruct.2012.12.029.

[8] B. Rosić, O. Pajonk, A. Litvinenko, and H. G. Matthies, *Sampling-free linear bayesian update of polynomial chaos represenations*, Journal of Computational Physics **231** (2012), no. 17, 5761–5787.

[9] A. Tarantola, *Inverse problem theory and methods for model parameter estimation*, SIAM, Philadelphia, 2004.

[10] L. Tierney, *Markov chains for exploring posterior distributions*, Ann. Statist. **22** (1994), no. 4, 1635–2134.

2.12 Nonlinear minimum mean square error estimation

Ansprechpartner:	Elmar Zander
EMail:	e.zander@tu-bs.de
Telefon:	0531/391-3011

A common problem in statistics with many interesting application is that of determining a minimum mean square error (MMSE) estimator. Let $\mathbf{X} : \Omega \to \mathbb{R}^n$ be a random vector of some unknown quantity and $\mathbf{Y} : \Omega \to \mathbb{R}^m$ a measurement expected to give some information about $\mathbf{X}$. An estimator $\boldsymbol{\varphi} : \mathbb{R}^m \to \mathbb{R}^n$ is any function of the measurements $\mathbf{Y}$. From these functions, the minimum mean square error estimator $\hat{\boldsymbol{\varphi}}$ is the one that minimises the mean square error defined by

$$e^2_{\text{MSE}} = \mathbb{E}[\|\mathbf{X}(\cdot) - \boldsymbol{\varphi}(\mathbf{Y}(\cdot))\|_2^2]. \tag{20}$$

It can be shown that the MMSE estimator $\hat{\boldsymbol{\varphi}}$ is the conditional expectation of $\mathbf{X}$ given the measurements $\mathbf{Y}$ [1, 2], i.e.

$$\hat{\boldsymbol{\varphi}}(\mathbf{Y}) = \mathbb{E}[\mathbf{X}|\mathbf{Y}], \tag{21}$$

making it nicely suitable for nonlinear Bayesian updating [3].

Since minimising over the whole space of measurable functions is numerically not possible in general, we will restrict the space to a finite dimensional function space $\mathcal{V}_{\boldsymbol{\varphi}}$ with basis functions Ψ_γ, indexed by some $\gamma \subset \mathcal{J}$ and $\mathcal{J}$ the set of indices. The functions Ψ_γ can be e.g. some sort of multivariate polynomials and the γ corresponding multiindices, but other function systems are also possible (e.g. tensor products of sines and cosines). An element $\boldsymbol{\varphi}$ of this function space has a representation as a linear combination

$$\boldsymbol{\varphi} := y \mapsto \sum_{\gamma \in \mathcal{J}} \boldsymbol{\varphi}_\gamma \Psi_\gamma(y). \tag{22}$$

of these basis functions.

The component functions φ_i of $\boldsymbol{\varphi}$ in (20) approximating X_i for $i \in [1 \dots n]$ are completely independent, and so the problem of computing the minimiser essentially factors into n independent problems and can be done component-wise. Minimising (20) for X_i and φ_i then becomes the same as solving

$$\frac{\partial}{\partial \varphi_{i,\delta}} \mathbb{E}[(X_i - \sum_\gamma \varphi_{i,\gamma} \Psi_\gamma(\mathbf{Y}))^2] = 0 \tag{23}$$

for all $\delta \in \mathcal{J}$. Using the linearity of the derivative operator and of the expectation leads to

$$\sum_\gamma \boldsymbol{\varphi}_{i,\gamma} \mathbb{E}[\Psi_\gamma(\mathbf{Y}) \Psi_\delta(\mathbf{Y})] = \mathbb{E}[X_i \Psi_\delta(\mathbf{Y})]. \tag{24}$$

This can be written as a linear system

$$\mathbf{A}\boldsymbol{\varphi}_i = \mathbf{b}_i \tag{25}$$

with $[\mathbf{A}]_{\gamma\delta} = \mathbb{E}[\Psi_\gamma(\mathbf{Y})\Psi_\delta(\mathbf{Y})]$, $[\mathbf{b}_i]_\delta = \mathbb{E}[X_i\Psi_\delta(\mathbf{Y})]$ and the coefficients $\boldsymbol{\varphi}_{i,\gamma}$ collected in the vector $\boldsymbol{\varphi}_i$. Note, that for the actual computation some linear ordering needs to be imposed on the indices $\gamma \in \mathcal{J}$, but this is not essential here and can be left to the implementation.

If the unknown $\mathbf{X}$ and the measurements $\mathbf{Y}$ are given by some GPC and the function space $\mathcal{V}_{\boldsymbol{\varphi}}$ consists of polynomials, the expectations could in principle be computed exactly using the GPC algebra. This is, however, computationally intensive (and non-trivial to do in addition to that). More efficient is to approximate $\mathbf{A}$ and $\mathbf{b}$ by numerical integration via

$$\mathbb{E}[\Psi_\gamma(\mathbf{Y})\Psi_\delta(\mathbf{Y})] \approx \sum_k w_k \Psi_\gamma(\mathbf{Y}(\xi_k))\Psi_\delta(\mathbf{Y}(\xi_k)) \tag{26}$$

and

$$\mathbb{E}[\mathbf{X}\Psi_\delta(\mathbf{Y})] \approx \sum_k w_k \mathbf{X}(\xi_k)\Psi_\delta(\mathbf{Y}(\xi_k)). \tag{27}$$

Choosing an integration rule of sufficient degree this can also be made exact.[1] In order to compute the estimator $\hat{\boldsymbol{\varphi}}$ now for a vector valued $\mathbf{X}$ the vectors $\boldsymbol{\varphi}_i$ and $\mathbf{b}_i$ can be collected into matrices and the whole system

$$\mathbf{A}[\boldsymbol{\varphi}_1, \cdots, \boldsymbol{\varphi}_n] = [\mathbf{b}_1, \cdots, \mathbf{b}_n] \tag{28}$$

solved at once, which sometimes makes the process more efficient.

2.12.1 Implementation

Instead of describing the foregoing algorithm in pseudo-code, an implementation in Matlab using the Stochastic Galerkin library sglib[?] will be presented. It can be seen that this implementation is not much longer than pseudo-code would be, and has the advantage of actually *running*.

- Line 4 generates the integration points ξ_k and weights w_k used in equations (26) and (27). Since no other options are given to `gpc_integrate`, the integration rule will be a Smolyak rule based on one-dimensional Gauss rules with respect to the measure given by the GPC germ in the GPC representation of $\mathbf{X}$ and $\mathbf{Y}$ (i.e. the vector of basic random variable in which $\mathbf{X}$ and $\mathbf{Y}$ are represented as polynomials of).
- Lines 7 and 8 evaluate $X_i(\xi_k)$ for $i = 1, \ldots, n$, $Y_j(\xi_k)$ for $j = 1, \ldots, m$.

[1] Suppose $\mathbf{Y}$ has total degree $p_{\mathbf{Y}}$ and $\boldsymbol{\varphi}$ has total degree $p_{\boldsymbol{\varphi}}$, then the maximum degree in the expression for $\mathbf{A}$ will be $2p_{\mathbf{Y}}p_{\boldsymbol{\varphi}}$ and a Gauss integration rule of order $p_{\mathbf{Y}}p_{\boldsymbol{\varphi}} + 1$ will suffice. For the computation of $\mathbf{b}$ a rule of order $\lceil (p_{\mathbf{X}} + p_{\mathbf{Y}}p_{\boldsymbol{\varphi}} + 1)/2 \rceil$ will suffice.

- Line 12 generates a representation of the function space $\mathcal{V}_\varphi$ as m-variate Chebyshev polynomials of the second kind (that is what the 'U' is for) up to complete degree p_φ.
- Lines 13 evaluates $\Psi_\gamma(\mathbf{Y}(\xi_k))$ for $\gamma \in \mathcal{J}$, i.e. the complete basis of $\mathcal{V}_\varphi$ for all $\mathbf{Y}(\xi_k)$ for.
- Line 16 compute $w_k \Psi_\gamma(\mathbf{Y}(\xi_k))$ for all k and γ, which is needed in both (26) and (27), making it more efficient to compute it once and store it.
- Lines 17 and 18 set up the matrix $\mathbf{A}$ and right hand side $\mathbf{b}$ according to Eqs. (26) and (27).
- Lines 19 solves the system Eq. (28). Note, that the transposes are necessary here, because otherwise δ would be the first index and i, contrary to the format generally used here.

```
1  function [phi_i_delta, V_phi]=mmse_estimate(x_func, ...
           y_func, V_x, p_phi, p_int)
2
3  % Generate integration points
4  [xi_k, w_k] = gpc_integrate([], V_x, p_int);
5
6  % Evaluate X and Y at the integration points
7  x_i_k = funcall(x_func, xi_k);
8  y_j_k = funcall(y_func, xi_k);
9
10 % Determine dimension of co-domain of Y and create
11 % function basis V_phi
12 m = size(y_j_k, 1);
13 V_phi=gpcbasis_create('U', 'm', m, 'p', p_phi);
14 Psi_gamma_k = gpcbasis_evaluate(V_phi, y_j_k);
15
16 % Compute matrix A and right hand side b and solve
17 Psiw_gamma_k = binfun(@times, Psi_gamma_k, w_k');
18 A = Psiw_gamma_k * Psi_gamma_k';
19 b = x_i_k * Psiw_gamma_k';
20 phi_i_delta = (A\b')';
```

Listing 1: Implementation of the nonlinear MMSE estimator using Matlab/sglib

Remark: An important point here is that, although φ is not actually a GPC (it does not directly represent a random quantity), it is a multivariate polynomial which shares many properties with GPC variables. Thus many of the GPC functions can be re-used here, which saves much effort in the implementation.

The following listing shows how the preceding code can be used for GPC variables, in which case the GPCs are just wrapped into callable functions.

```
function [phi_i_delta, V_phi]=mmse_estimate_gpc(...
        x_i_alpha, V_x, y_j_beta, V_y, p_phi, p_int)

% Generate functions from the GPC bases and coeffs
x_func = gpc_function(x_i_alpha, V_x);
y_func = gpc_function(y_j_beta, V_y);

% Call the MMSE estimator function
[phi_i_delta, V_phi]=mmse_estimate(x_func, y_func, V_x...
        , p_phi, p_int);
```

Listing 2: Implementation of the nonlinear MMSE estimator for GPCs

2.12.2 Examples

The following examples have been constructed by artificially generating GPC expansions for $\mathbf{X}$ and $\mathbf{Y}$ by randomly generating coefficients for n, respectively m, generalised polynomial chaoses in d random variables, up to some total degree p_x and p_y. The nonlinear MMSE was then used to approximate the "unknown" random vector $\mathbf{X}$ by the "measurements" $\mathbf{Y}$.

Figure 22 shows the nonlinear MMSE for $d = m = n = 2$ and different values of $p_{\boldsymbol{\varphi}}$, the polynomial degree of $\boldsymbol{\varphi}$. Since $d = m$ the estimator can be expected to converge for large values of $p_{\boldsymbol{\varphi}}$, i.e. $\lim_{p_{\boldsymbol{\varphi}}\to\infty} \|\mathbf{X} - \hat{\boldsymbol{\varphi}}(\mathbf{Y}; p_{\boldsymbol{\varphi}})\| = 0$. This can be seen in the figures by noting that the crosses (x), denoting the approximated values $\hat{\mathbf{X}} = \hat{\boldsymbol{\varphi}}(\mathbf{Y}; p_{\boldsymbol{\varphi}})$, are increasingly better centred in the circles (o), denoting the true values of $\mathbf{X}$, in the sequence of increasing $p_{\boldsymbol{\varphi}}$.

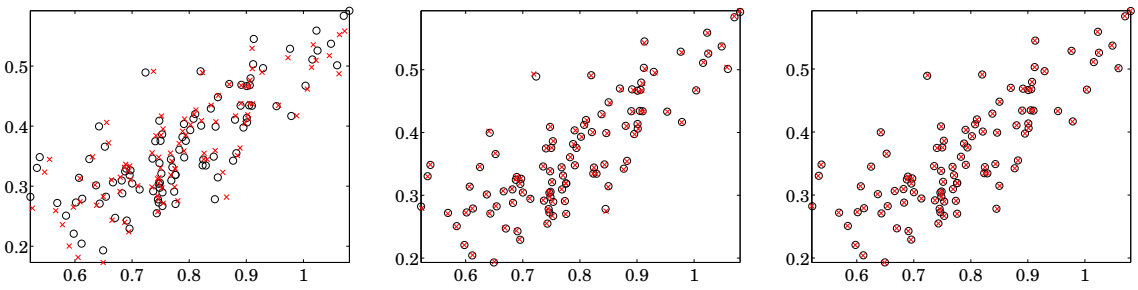

Figure 22: MMSE estimation with increasing polynomial degrees $p_{\boldsymbol{\varphi}} = 1$, 2, and 3 from left to right (for $m = n = d = 2$). True values $\mathbf{X}$ are marked by o, and estimated values $\hat{\mathbf{X}} = \boldsymbol{\varphi}(\mathbf{Y})$ are marked by x.

In the two leftmost graphs in Figure 23 one can see the MMSE estimation with $n = d = 2$, like in the previous example, but only one

measurement ($m = 1$). Of course, the estimate can be only a one-dimensional submanifold, which is in the left figure for $p_{\varphi} = 1$ an affine subspace. For $p_{\varphi} = 3$ in the middle figure the estimate is nonlinear, and matches better the shape of the original distribution.

In the rightmost figure the parameters are $m = n = 3$, $d = 5$ and $p_{\varphi} = 4$. Even though, the number of measurements is the same as the number of variables to estimate and the polynomial degree is relatively high, there is no convergence, since the number of "hidden" parameters d is higher than m, and so no convergent approximation can be expected.

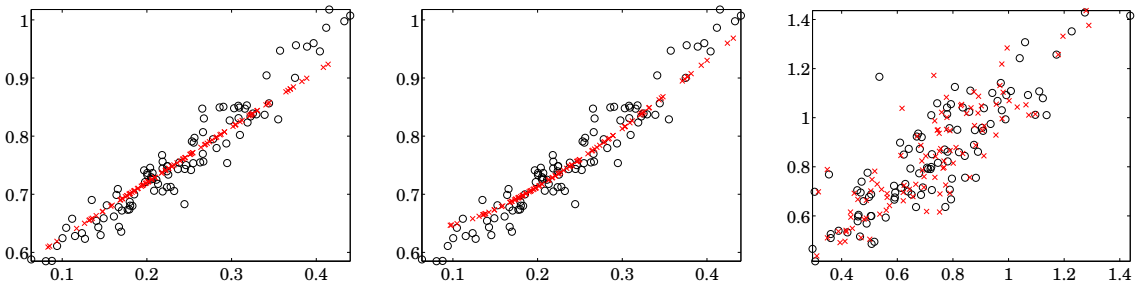

Figure 23: MMSE estimation with $m = 1, p_{\varphi} = 1$ (left), $m = 1, p_{\varphi} = 3$ (middle), and $m = 3, d = 5, p_{\varphi} = 4$ (right). True values $\mathbf{X}$ are marked by o, and estimated values $\hat{\mathbf{X}} = \varphi(\mathbf{Y})$ are marked by x.

2.12.3 Outlook

The foregoing method has large potential to be used as a basis for nonlinear Bayesian updating, as the basis functions can be arbitrary. Further applications currently under investigation are for recompression of PC expansions, which can be formulated as minimisation problems over the mean square error on rotated PC germs, making it necessary to perform the minimisation over the product manifold of the coefficient space times a Grassmann manifold.

References

[1] D. P. Bertsekas and J. N. Tsitsiklis, *Introduction to probability*, 2 ed., Athena Scientific, 2008.

[2] A. Oppenheim and G. Verghese, *Introduction to Communication, Control and Signal Processing*, Online (MIT OpenCourseWare), URL: http://bit.ly/1eWIUrR.

[3] B. Rosić, O. Pajonk, A. Litvinenko, and H. G. Matthies, *Sampling-free linear Bayesian update of polynomial chaos represenations*, Journal of Computational Physics **231** (2012), no. 17, 5761–5787.

2.13 Hydrological extreme events analysis for flood risk mitigation

Ansprechpartner:	Valentina Chiarello
EMail:	valentina.chiarello@dicea.unifi.it
Telefon:	+39-055-4796306 and 0531/391-3009

2.13.1 Introduction

Extreme river floods have been a substantial natural hazard over the past centuries, and now the impacts of human activities are leading to changes in the magnitudes and frequency of floods even at remote locations. In this framework, considerable attention has been given in the last decades in studying, understanding, and predicting the nature of environmental extreme events. The general idea of the research activity is to estimate the best flood risk management strategy considering that it should be effectively combined also with water resources management and policy implementation. In engineering practice the knowledge of peak flow discharges is of primary importance for the planning of water resources and risk assessment. The aim is to provide and implement a new predictive model that may be useful to assess the desired stream flow index even in ungauged river basins.

2.13.2 Methodology

According to the Prediction in Ungauged Basin - PUB science initiative promoted by the International Association of Hydrological Science - IAHS [10], hydrologists have developed numerous predictive tools such as empirical models, lumped models, distributed models and statistical regionalizations to predict runoff in ungauged catchments. The estimation of the extreme stream flow related variables in ungauged river basins and in sites characterized by short or discontinuous time series has been mainly based on regional regression techniques, relating streamflow statistics and geomorphoclimatic basin characteristics. Regional analysis is the classical approach to estimate river flow characteristics at sites where little or no data exists. The two main steps of the regional analysis are the identification of groups of hydrologically homogeneous regions and the application of a regional estimation method within each delineated region. Recently, geostatistic spatial interpolation techniques, which allow estimation of a variable including its uncertainty at locations where no measurements are available, have been proposed for regionalizing the desired stream flow index. A method of geostatistical estimation on stream networks known as Top-kriging, or topological kriging is proposed in [11]. The method is a kriging interpolation procedure that takes

into account the geometric organization and structure of a hydrographic network, the catchment area and the stronger spatial correlation between nested catchments. The authors exploited also short records taking into account local uncertainties of the measurements that may differ between locations, providing the estimation of predictive uncertainty in ungauged catchments. Another approach for regional flood frequency estimation, termed canonical kriging (CK), or physiographical-space-based interpolation (PSBI), is presented in [4]. This methodology, using physiographical and meteorological characteristics of gauging stations and multivariate analysis techniques such as principal components analysis (PCA) and canonical correlation analysis (CCA), interpolates flow quantiles with Ordinary kriging through the continuous physiographical space (physiographical space-based kriging method). PSBI with Top-kriging for low flow predictions in ungauged sites, observing the complementary utility of the two methods for headwater and larger scale catchments is compared in [3]. Implicitly, the authors suggested the possibility of improving the prediction accuracy by blending the two methods but the analysis performed in [1] shown that coupling Top-Kriging with CK slightly improves the flood quantile predictions in ungauged sites. These applications of spatial interpolation techniques to regionalization of streamflow regime share a common background idea: both perform a smooth regionalization of streamflow indices seamlessly over the stream network (Top-kriging) or the physiographical space (PSBI) without identifying groups of hydrologically homogeneous regions. Traditional methods for regional flood frequency analysis at ungauged sites are built upon the assumption that the hydrologic regime does not vary through time (i.e. stationary). Non-stationarity in the hydrologic regime can be induced by changes in the climatology but also in the drainage basin characteristics. A non-stationary regional model, an alternative approaches that take non-stationarity into account, is presented in [7]. In a most recent work [8], a modified version of the original PSBI method, based on residual kriging (RK) in physiographical space, is proposed for regional flood frequency analysis. In this approach, in order to remove any possible spatial trends within the hydrological variables over the physiographical space, the trend is quantified and removed from the hydrological variable. Prediction of runoff in ungauged river basins is notoriously a difficult task because the tremendous spatio-temporal heterogeneity of climatic and landscape properties involve significant unknowns and uncertainties. However, it is increasingly acknowledged that spatial proximity does not necessarily entail similarity in functional behaviour. To define more significant metrics or dissimilarity measures for predicting flow, in [9]] it is suggested to use pair-wise empirical copula densities. Copulas have received increasing attention as a spatial analysis tool, as

a better alternative to the traditional geostatistics for spatial modeling [2], [6], and for modelling dependence in space and time [5].

2.13.3 Definition of the study area and dataset description

The case study is defined by the rainfall data and discharges data, recorded in several rivers in the Tuscany Region, having an area of about 23000 km^2. The time series of annual maxima of peaks discharges recorded in the period 1923-2011, have been collected. The time series of annual maxima of rainfall depth for short duration of 1, 3, 6, 12, and 24 h, recorded from 1916 to 2012 at 540 rain gauges, have been collected and validated. The rainfall database consists also of the annual maximum values of the daily rainfall measured at 795 raingauges over the same years.

2.13.4 Future works

In order to improve the capability to predict stream flow indices in ungauged sites, Top-kriging and residual kriging will be applied. As alternative to the geostatistic techniques for spatial modeling, Copulas will be used as a spatial analysis tool. Finally, quantification of the accuracy of the different interpolation techniques and development of the most suitable procedure for defining the best flood risk management strategy will be realized.

References

[1] S. A. Archfield, A. Pugliese, A. Castellarin, J. O. Skøien, and J. E. Kiang, *Topological and canonical kriging for design flood prediction in ungauged catchments: an improvement over a traditional regional regression approach?*, Hydrology and Earth System Sciences (2013), no. 17, 1575–1588.

[2] A. Bárdossy and J. Li, *Geostatistical interpolation using copulas*, Water Resources Research **44** (2008), no. W07412.

[3] S. Castiglioni, A. Castellarin, A. Montanari, J. O. Skøien, G. Laaha, and G. Blöschl, *Smooth regional estimation of low-flow indices: physiographical space based interpolation and top-kriging*, Hydrology and Earth System Sciences (2011), no. 15, 715–727.

[4] K. Chokmani and T. Ouarda, *Physiographical space-based kriging for regional flood frequency estimation at ungauged sites*, Water Resources Research **40** (2004), no. W12514.

[5] B. Gräler and E. Pebesma, *The pair-copula construction for spatial data: a new approach to model spatial dependency*, Procedia Environmental Sciences **7** (2008), 206–211.

[6] H. Kazianka and J. Pilz, *Bayesian spatial modeling and interpolation using copulas*, Computers & Geosciences **37** (2011), 310–319.

[7] M. Leclerc and T. Ouarda, *Non-stationary regional flood frequency analysis at ungauged sites*, Journal of Hydrology (2007), no. 343, 254–265.

[8] M. K. Nezhad, K. Chokmani, T. B. M. J. Ouarda, M. Barbet, and P. Bruneau, *Regional flood frequency analysis using residual kriging in physiographical space*, Hydrological Processes **24** (2010), 2045–2055.

[9] L. Samaniego, A. Bárdossy, and R. Kumar, *Streamflow prediction in ungauged catchments using copula-based dissimilarity measures*, Water Resources Research **46** (2010), no. W02506.

[10] M. Sivapalan, K. Takeuchi, S. Franks, V. Gupta, H. Karambiri, V. Lakshmi, X. Liang, J. McDonnell, E. Mendiondo, P. O'Connell, T. Oki, J. Pomeroy, D. Schertzer, S. Uhlenbrook, and E. Zehe, *IAHS Decade on Predictions in Ungauged Basins (PUB), 2003-2012: Shaping an exciting future for the hydrological sciences*, Hydrological Sciences Journal **48** (2003), no. 6, 857–880.

[11] J. Skøien, R. Merz, and G. Blöschl, *Top-kriging — geostatistics on stream networks*, Hydrology and Earth System Sciences (2006), no. 10, 277–287.

2.14 Seismic risk analysis for Hospital structures

Ansprechpartner:	Alberto Ciavattone
EMail:	alberto.ciavattone@dicea.unifi.it
Telefon:	+39-055-4796326 or 0531/391-3009

Italy is a territory characterized by a high seismic risk, which is a function of three main aspects: seismic hazard of the territory, vulnerability of the structure and exposure.

The assessment of the structural vulnerability for existing buildings is a key aspect for the seismic risk reduction, in particular for strategic and relevant buildings, because of their importance for the civil protection.

There are different approaches for the evaluation of the structural vulnerability: expeditious empirical methods, based on qualitative evaluations, analytical methods, based instead on detailed models, and hybrid methods, combination of the first two methods.

In case of a large sample of buildings (as the Hospital structures of the cities of Florence, Prato and Pistoia, sample of analysis of the present work, composed both from masonry and reinforced concrete structures), a first screening in terms of vulnerability must be performed with an expeditious empirical approach, in order to highlight the most vulnerable objects and, as a consequence, to decide which buildings analyze at first with detailed analyses [3]. It is clear that a detailed investigation for all the structures of a large sample of buildings is not possible at first, due to the limited resources of the Administrations.

One of these empirical methods has been applied to the sample: the Vulnerability Index Method, originally proposed by Benedetti and Petrini [1], allows the estimation of an Index of Vulnerability in the range 0%–100%, where high values correspond to high vulnerable structures; the index has been estimated for each structure simply evaluating, in a qualitative way, 11 parameters related to the features of the building itself, both from the structural and non structural point of view [4].

The statistical results of this approach give general information about the sample: it has been possible to observe, for example, the general distribution of Vulnerability of the entire sample (219 buildings), or the influence of the age of construction on the Vulnerability Index (see Fig. 24).

Then, focusing on the masonry structures of the sample (118 buildings), a comparison among the results of the Vulnerability Index Method and the detailed analytical analyses on a subset of structures (20 buildings) has been performed, showing that there is a relation among them,

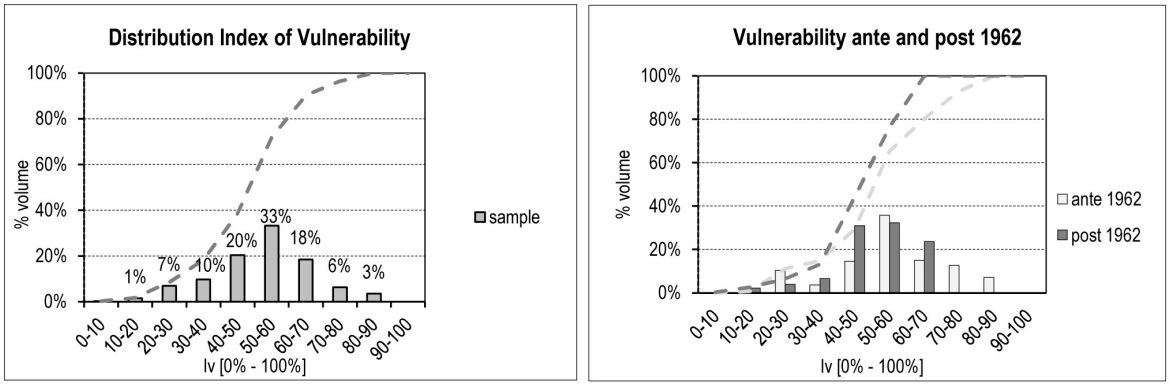

Figure 24: Some statistical results of the application of the Vulnerability Index Method on the sample.

which can be used in order to obtain more information about the behaviour of the structures: in fact, the empirical approach gives as result only a Vulnerability Index in the range 0%–100%, while the detailed analyses, studying the behaviour of a three dimensional non-linear model, can give some indicators of the seismic risk for the considered structure.

The detailed studies have been performed on three dimensional models of the structures, using the Frame by Macro Element (FME) approach [2], where each element of the building (piers and spandrel beams) has a non linear behaviour. The static non linear analysis procedure has been used [5], obtaining the pushover curves (8 for each structure) and calculating the related minimum peak ground acceleration of capacity PGAc (see Fig 25).

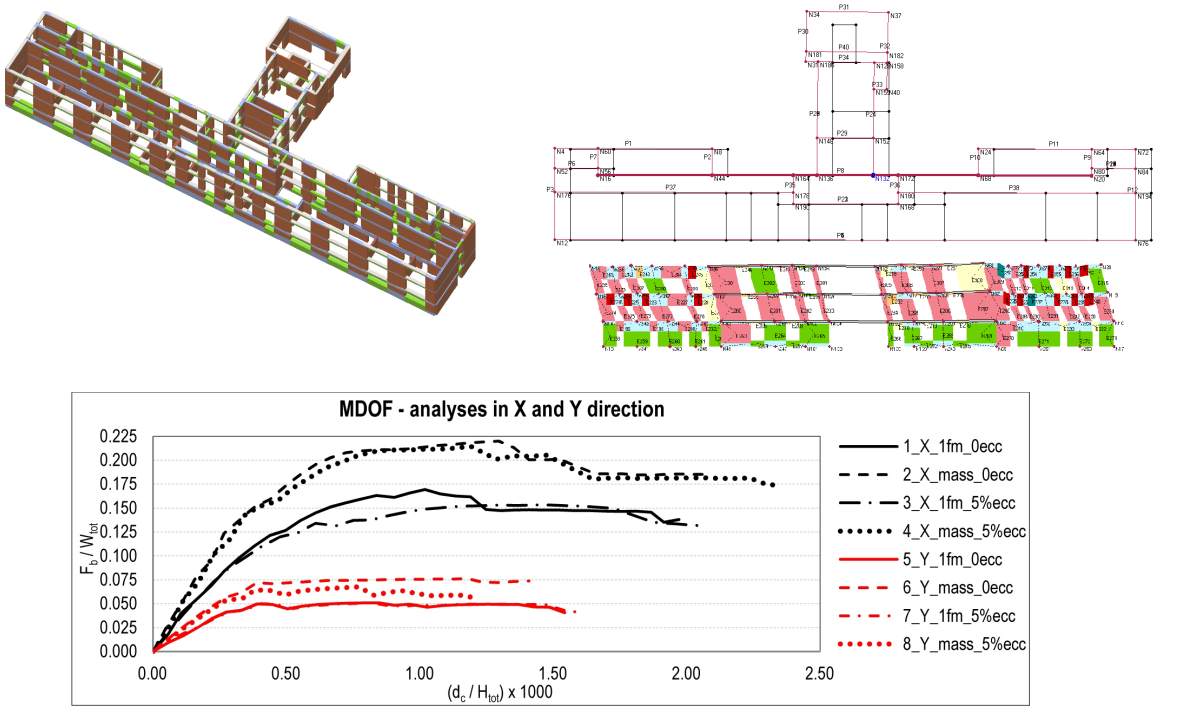

Figure 25: Three dimensional model of a structure, example of pushover analysis in longitudinal direction and pushover curves obtained for all the analyses.

The comparison among the two approaches has highlighted a rela-

tion, which can be observed in Fig. 26: high values of Index of Vulnerability Iv correspond to low values of capacity, expressed in terms of PGAc, as well as low values of Iv lead to high values of PGAc.

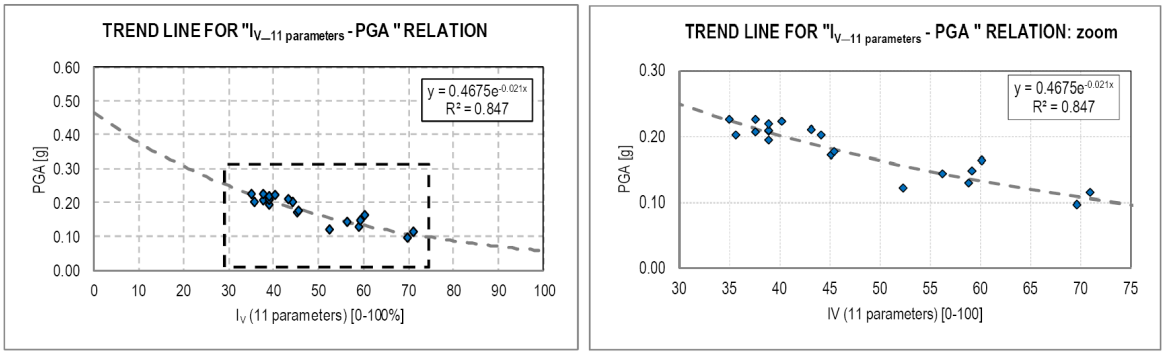

Figure 26: Relation among the expeditious method (Iv) and the detailed one (PGAc) for the vulnerability evaluation.

Starting from this, the relation among the two approaches has been studied, using only the parameters of the empirical method which are referred to the structural global behaviour, making in this way the comparison more direct: the level of relation increases, since the two methods consider the same elements in their analyses.

Before starting to design a new expeditious vulnerability assessment method, each singular parameter of the original Vulnerability Index Method has been analyzed, observing the influence of each of them in the estimation of the Index and evaluating the relation with the other parameters: most of them are completely independent, even if some relations can be observed due to technological reasons.

After this analysis, a proposal of a new vulnerability assessment method has been done, specifically conceived for masonry structures: this new method requires the same amount of information necessary for the Vulnerability Index Method and it allows the estimation of the peak ground acceleration of capacity PGAc related to the global behaviour of the structure, using a simple linear equation (obtained through a multi-linear regression) and the evaluation of a reliability index of the capacity estimation mentioned above, in order to consider the possibility of occurrence of local mechanisms collapses.

The estimation of the capacity of the structure, expressed in terms of PGAc, can be performed considering four main aspects: the lateral resistant indicator, parameter obtained from the product among the shear resistance of the material of construction and the quantity of masonry piers (normalized to the global surface of the representative level of the building for the shear capacity), the typologies of floors and roof, the planimetric and elevation configuration. The first parameter is quantitative, while the other ones are qualitative: the multi-linear regression

keeps into account the contribution of each of them through a weighted sum, which gives as result directly the acceleration of capacity of the considered structure, supposing the possibility of global behaviour of it.

With this estimation, it is possible to obtain a first index of seismic risk, simply considering the ratio among the capacity value and the demand one, dependent from the site of construction seismic hazard and the geotechnical conditions.

The required information for this method is the same of the original Vulnerability Index Method: the Index of Vulnerability can be calculated even in this case, since it is a useful instrument for the creation of a first general vulnerability classification, considering both structural (global and local behaviour) and non structural aspects. The new proposed method provides more information of the original one, giving numerical estimations of the capacity of the considered structures and allowing the calculation of indexes of risk.

References

[1] D. Benedetti and V. Petrini, *Sulla vulnerabilità di edifici in muratura: proposta di un metodo di valutazione*, L'industria delle Costruzioni **149** (1984), no. 1, 66–74.

[2] A. Galasco, S. Lagomarsino, and A. Penna, *TREMURI program: Seismic analyser of 3D masonry buildings*, Tech. report, University of Genoa, 2002.

[3] D. Grant, J. Bommer, R. Pinho, and G. Calvi, *Defining priorities and timescales for seismic intervention in school buildings in Italy*, Research Report Rose – 2006/03, IUSS Press, Pavia, Italy, 2006.

[4] Gruppo Nazionale per la Difesa dai Terremoti, *Rischio sismico di edifici pubblici, parte I: aspetti metodologici*, Proceedings of C.N.R.-Gruppo Nazionale per la Difesa dai Terremoti, Roma, Italia, 1993.

[5] Decreto Ministeriale Infrastrutture del 14/01/2008, *Nuove norme tecniche per le costruzioni*, 2008.

2.15 Dynamic behavior of mooring lines for floating offshore wind turbines

Ansprechpartner:	Giovanni Stabile
EMail:	giovanni.stabile@dicea.unifi.it
Telefon:	+39-055-4796306 or+39-333-5273567

2.15.1 Motivation

In the last years several advances in the wind energy sector have led to the building of a number of offshore wind turbines,although most of them are either on-shore or are being erected on a fixed-bottom support structure in relatively shallow waters near the cost. A large part of the global wind resource is located in deeper waters where fixed-bottom structures become not economically feasible. Floating wind turbine platforms may be the most economical means for placing offshore wind turbines in deeper water. In order to realize a technology that can compete with other energy sources the development of cost-effective designs is needed. Therefore there is the need to develop reliable tools which can model the dynamics and the response of floating wind turbine platforms in a comprehensive and fully integrated manner. Previous research has demonstrated the technical feasibility of floating wind turbines using frequency-domain analysis. Frequency domain calculations are easier to develop and need less computational resources in respect to time-domain calculations. However frequency-domain calculations have some important limitations because they cannot accurately represent non-linear dynamic characteristics or model transient loading events. Thus to obtain a reliable and cost-effective design a tool which can analyze various configurations of the wind turbine platform in time-domain is needed.

Aspects regarding the modeling of floating offshore wind turbine can be subdivided into four main topics:

- Structural Dynamics
- Rotor Aerodynamics
- Platform Hydrodynamics
- Mooring Lines

The dynamics of mooring lines, among these aspects, is certainly one that requires further developments [2].

2.15.2 Numerical Methods

In order to study the dynamics of cable undergoing large displacements and deformations, the development of a geometrically exact beam model

is needed. The geometrically exact beam theory has been proposed for the first time by Reissner [6] but his formulation was really exact only for the 2-D case. The theory of Reissner has been extended for the 3-D case by Simo [7] and its finite element formulation for the static case has been given by Simo & Vu-Quoc [8]. A finite element formulation for the dynamic case has been given for the first time by Simo & Vu-Quoc [9]. Cardona and Geradin [1] give another finite element implementation for the geometrically exact beam theory and they named the formulations, depending on the different updating procedures, as Eulerian, total Lagrangian and updated Lagrangian. In the same article they give also the implementation for an updated Lagrangian formulation. A total Lagrangian formulation for the static case has been proposed by Ibrahimbegovic et al [3] while several updated and Eulerian formulations for dynamic cases have been proposed by Ibrahimbegovic & Al Mikdad [4]. A total Lagrangian formulation for the dynamic case, which can bypass the singularity which arises at the rotation angle of 2π has been proposed by Mäkinen [5].

It has been used a geometrically exact beam theory with a total Lagrangian formulation. The formulation is based on the one proposed by Mäkinen [5]. This approach permits to consider finite shearing, extension, flexure and torsion. As already stated, a beam-theory is assessed as geometrically exact if no other kinematic assumptions during the derivation are assumed than the basic kinematic assumptions. In this approach the cross section remain plane and undeformed during the deformation processes and can only rotate as a rigid body. The shear strain is included within this theory, it means that the cross sections, during the rotation, do not necessarily remain perpendicular to the line of centroids. The configuration of the beam is described by means of the position vector, which describes the position of the line of centroids respect to the reference system, and by means of the rotation tensor, which describes the rotation of the cross sections respect to the reference system. Three-dimensional rotations are treated making usage of the Euler-Rodrigues parametrization which gives the relationship between the rotation vector and the rotation tensor. This approach, since no approximations are introduced. permits to describe accurately the kinematic of the beam and the relative measures of strain and stress. With such assumptions on the kinematics the beam equations of motion are written and an appropriate weak form for the numerical implementation is developed. The total Lagrangian formulation, which refers always to the initial configuration, bypassing the singularity for rotation angles of 2π with a change of paremetrization, since rotation vectors at different instants belong to the same vector space, permits the usage of a standard Newmark algorithm for the time integration. The spatial discretization is based on

the standard Galerkin isoparametric finite element approximation of the variatonal equation of the virtual work. This procedure provides, at each time step, a non-linear algebraic system of equations which is solved using an iterative Newton-Raphson method. Parts of the structure which belong to different systems are coupled together, with suitable joints, using a master-slave approach.

2.15.3 Future Work

The global model, formed by rotor, hub, tower, platform and mooring lines will be coupled with a fully hydrodynamic solver which is able to simulate also severe load conditions. The hydrodynamic solver is based on the fully nonlinear potential flow theory where the Laplace equation is solved using a boundary element method. This approach permits to consider also higher order phenomena which may be important for the structural modelling. Moreover it permits to model severe load conditions which are not considered within linear and second order theories. The coupling between the structural and hydrodynamic model, since the structure is composed mainly by slender bodies, can be performed using Morison equation which permits to consider also viscous effects.

References

[1] A. Cardona and M. Geradin, *A Beam Finite Element Non-Linear Theory with Finite Rotations*, International Journal for Numerical Methods in Engineering **26** (1988), 2403–2438.

[2] A. Cordle, *State of the Art in Floating Wind Turbine Design Tools*, International Offshore and Polar Engineering Conference, 2011.

[3] A. Ibrahimbegović, *On finite element implementation of geometrically nonlinear Reissner's beam theory: three-dimensional curved beam elements*, Computer methods in applied mechanics and . . . **7825** (1995), no. 95, URL: http://www.sciencedirect.com/science/article/pii/004578259500724F.

[4] A. Ibrahimbegović and M. Mikdad, *Finite rotations in dynamics of beams and implicit time-stepping schemes*, International Journal for . . . **41** (1998), no. November 1996, 781–814.

[5] J. Mäkinen, *A Formulation for Flexible Multibody Mechanics*, butler.cc.tut.fi (2004), no. December, URL: http://butler.cc.tut.fi/~jmamakin/vk.pdf.

[6] E. Reissner, *On one-dimensional large-displacement finite-strain beam theory*, Studies in applied mathematics

(1973), URL: http://siba.unipv.it/fisica/articoli/S/StudiesinAppliedlMathematics_vol.52_no.2_1973_pp.87-95.pdf.

[7] J. Simo, *A finite strain beam formulation. The three-dimensional dynamic problem. Part I*, Computer methods in applied mechanics and ...(1985), URL: http://scholar.google.com/scholar?hl=en&btnG=Search&q=intitle:A+finite+strain+beam+formulation.+The+three-dimensional+dynamic+problem.+Part+I#0.

[8] J. Simo and L. Vu-Quoc, *A three-dimensional finite-strain rod model. Part II: Computational aspects*, Computer methods in applied mechanics and ...(1986), URL: http://www.sciencedirect.com/science/article/pii/0045782586900794.

[9] J. Simo and L. Vu-Quoc, *On the dynamics in space of rods undergoing large motions — a geometrically exact approach*, Computer methods in applied mechanics and ...(1988), URL: http://www.sciencedirect.com/science/article/pii/0045782588900734.

3 Lehre im WS 2012/2013 and SS 2013

3.1 Wintersemester 2012/2013

Advanced Object Oriented C++ Techniques	2+2	Rainer Niekamp
Seminar zum wissenschaftlichen Rechnen	0+2	Hermann G. Matthies, Elmaz Zander
Weiterführendes Programmieren/ Intermediate Programming	0+4	Hermann G. Matthies, Rainer Niekamp
Einführung in das Programmieren (für Nicht-Informatiker)	0+4	Hermann G. Matthies, Rainer Niekamp
Einführung in das Wissenschaftliche Rechnen (ODE I)	2+1	Hermann G. Matthies, Joachim Rang
Einführung in das Parallele Rechnen	2+1	Thorsten Grahs
Visualisierung wissenschaftlicher Daten	2+1	Joachim Rang
Bionische Methoden der Optimierung I	2+1	Joachim K. Axmann, Oliver Pajonk
Einführung in PDE und Numerische Methoden für PDEs	2+1	Hermann G. Matthies, Alexander Litvinenko
Praktikum zum Wissenschaftlichen Rechnen	0+4	Alexander Litvinenko
Refresher Kurse für Mathematik und Matlab		Joachim Rang und Elmar Zander

3.2 Sommersemester 2013

Fortgeschrittene Methoden für ODEs und DAEs	2+1	Hermann G. Matthies, Joachim Rang
Uncertainty Quantification, Parametric Problems, and MOR	2+1	Hermann G. Matthies
Partitioned Methods for Multifield Problems	2+1	Joachim Rang, Martin Krosche
Advanced Object Oriented C++ Techniques	2+2	Rainer Niekamp
Seminar zum wissenschaftlichen Rechnen	0+2	Hermann G. Matthies, Elmar Zander
Weiterführendes Programmieren/ Intermediate Programming	0+4	Hermann G. Matthies, Rainer Niekamp
Einführung in das Programmieren (für Nicht-Informatiker)	0+4	Hermann G. Matthies, Rainer Niekamp
Praktikum zum Wissenschaftlichen Rechnen	0+4	Hermann G. Matthies, Alexander Litvinenko
Software Entwicklungspraktikum	0+4	Hermann G. Matthies, Elmar Zander
Parallel Computing I	3+1	Thorsten Grahs

4 Veröffentlichungen und Vorträge

4.1 Schriften und Proceedings

[1] M. Espig, W. Hackbusch, A. Litvinenko, H. G. Matthies, and E. Zander, *Efficient analysis of high dimensional data in tensor formats*, Sparse Grids and Applications (J. Garcke and M. Griebel, eds.), Lecture Notes in Computational Science and Engineering, vol. 88, Springer Berlin Heidelberg, 2013, pp. 31–56, doi:10.1007/978-3-642-31703-3_2.

[2] N. Friedman, M. Weiner, Gy. Farkas, I. Hegedűs, and A. Ibrahimbegović, *On the snap-back behavior of a self-deploying antiprismatic column during packing*, Engineering Structures **50** (2013), 74–89, doi:10.1016/j.engstruct.2012.12.035.

[3] N. Friedman and A. Ibrahimbegović, *Overview of highly flexible, deployable lattice structures used in architecture and civil engineering undergoing large displacements*, Ybl Journal of Built Environment **1** (2013), no. 1, 85–103, doi:10.2478/jbe-2013-0006.

[4] N. Friedman, V. Pomezanski, and E. Pintér, *George Rozvany and Tomasz Lewinski (eds): Topology optimization in structural and continuum mechanics*, Struct. Multidisc. Optim. **48** (2013), 1027–1029, doi:10.1007/s00158-013-1007-5.

[5] M. Hadigol, A. Doostan, H. G. Matthies, and R. Niekamp, *Partitioned treatment of uncertainty in coupled domain problems: A separated representation approach*, (2013), URL: arXiv:1305.6818[math.PR].

[6] M. Krosche, *A generic component-based software architecture for the simulation of probabilistic models*, Ph.D. thesis, Technische Universität Braunschweig, Braunschweig, 2013, URL: http://www.digibib.tu-bs.de/?docid=00052792.

[7] A. Litvinenko and H. G. Matthies, *Numerical methods for uncertainty quantification and Bayesian update in aerodynamics*, Management and Minimisation of Uncertainties and Errors in Numerical Aerodynamics (B. Eisfeld, H. Barnewitz, W. Fritz, and F. Thiele, eds.), Notes on Numerical Fluid Mechanics and Multidisciplinary Design, vol. 122, Springer Berlin Heidelberg, 2013, pp. 265–282, doi:10.1007/978-3-642-36185-2_11.

[8] A. Litvinenko, H. G. Matthies, and T. A. El-Moselhy, *Sampling and low-rank tensor approximation of the response surface*, Monte Carlo and Quasi-Monte Carlo Methods 2012 (J. Dick, F. Y. Kuo, G. W.

Peters, and I. H. Sloan, eds.), Springer Proceedings in Mathematics and Statistics, vol. 65, Springer Berlin Heidelberg, 2013, pp. 535–551, doi:10.1007/978-3-642-41095-6_27.

[9] E. D. Monte, A. Borghini, A. Ciavattone, B. Ortolani, and A. Vignoli, *Analisi della vulnerabilità sismica degli edifici ospedalieri situati in tre province della regione toscana*, Atti del XV ANIDIS 2013 „L'Ingegneria Sismica in Italia", Padova, Italy, 2013, URL: http://convegno.anidis.it/index.php/anidis/2013/schedConf/presentations.

[10] O. Pajonk, B. V. Rosić, and H. G. Matthies, *Sampling-free linear Bayesian updating of model state and parameters using a square root approach*, Computers & Geosciences (2013), no. 55, 70–83, doi:10.1016/j.cageo.2012.05.017.

[11] J. Rang, *Adaptive timestep control for the generalised-α method*, Adaptive Modelling and Simulation (D. Aubry, P. Diez, B. Tie, and N. Paréz, eds.), CIMNE, Barcelona, 2013, pp. 559–570, URL: http://www.lacan.upc.edu/admos2013/proceedings/ADMOS_2013_EBOOK.pdf.

[12] J. Rang, *An analysis of the Prothero-Robinson example for constructing new DIRK and ROW methods*, Journal of Computational and Applied Mathematics, published online (2013), doi:http://dx.doi.org/10.1016/j.cam.2013.09.062.

[13] J. Rang, *Coupling generalised-α methods: Analysis, adaptivity, and numerics*, Computational Methods for Coupled Problems in Science and Engineering V. A Conference Celebrating the 60th Birthday of Eugenio Oñate, 17-19 June 2013, Santa Eulalia, Ibiza, Spain (M. P. S. Idelsohn and B. Schrefler, eds.), CIMNE, Barcelona, 2013, pp. 399–401, URL: http://congress.cimne.com/coupled2013/frontal/doc/Coupled13_ebook.pdf.

[14] J. Rang and H. G. Matthies, *Stochastic Navier-Stokes equations are a coupled system*, Computational Methods in Marine Engineering V, Proceedings Marine 2013, Hamburg (B. B. und Peter Wriggers, ed.), CIMNE, Barcelona, 2013, pp. 399–401, URL: http://congress.cimne.com/marine2013/frontal/doc/Ebook-Marine2013.pdf.

[15] B. Rosić, *Variational formulations and functional approximation algorithms in stochastic plasticity of materials*, Proceedings of the Second ECCOMAS Young Investigators Conference 2013, Bordeaux, France, 2013, URL: http://hal.archives-ouvertes.fr/docs/00/85/58/38/PDF/RosicYIC2013.pdf.

[16] B. Rosić, A. Kučerová, J. Sýkora, O. Pajonk, A. Litvinenko, and H. Matthies, *Parameter identification in a probabilistic setting*, Eng. Struct. **50** (2013), no. 1, 179–196, doi:10.1016/j.engstruct.2012.12.029.

[17] B. Rosić and H. G. Matthies, *Identification of properties of stochastic elastoplastic systems*, Computational Methods in Stochastic Dynamics (M. Papadrakakis, G. Stefanou, and V. Papadopoulos, eds.), Computational Methods in Applied Sciences 26, Springer-Verlag, Dordrecht, 2013, pp. 237–253, URL: http://www.springer.com/materials/mechanics/book/978-90-481-9986-0.

4.2 Berichte

[1] L. Giraldi, A. Litvinenko, D. Liu, H. G. Matthies, and A. Nouy, *To be or not to be intrusive? The solution of parametric and stochastic equations – the plain vanilla Galerkin case*, Informatikbericht 2013-03, TU Braunschweig, Braunschweig, 2013, URL: http://www.digibib.tu-bs.de/?docid=00053932.

[2] M. Krosche and W. Heinze, *An aircraft design with uncertain parameters: A robustness analysis through a component-based software system*, SFB 880 — Fundamentals of High-Lift for Future Commercial Aircraft, Biennial Report, CFF Forschungsberichte, no. 2013–03, TU Braunschweig — Campus Forschungsflughafen, Braunschweig, 2013, pp. 191–203.

[3] A. Litvinenko and H. G. Matthies, *Sampling and low-rank tensor approximations*, Tech. report, Oberwolfach Report 4/2013 to Workshop Numerical Methods for PDE Constrained Optimization with Uncertain Data, 2013.

[4] A. Litvinenko, H. G. Matthies, and B. Khoromskij, *Data sparse approximation of the Karhunen-Loéve expansion*, Tech. report, Oberwolfach Report to Miniworkshop Numerical Upscaling for Media with Deterministic and Stochastic Heterogeneity, 2013.

[5] H. G. Matthies, A. Litvinenko, B. V. Rosić, A. Kučerová, J. Sýkora, and O. Pajonk, *Stochastic setting for inverse identification problem*, Tech. report, Oberwolfach Report 4/2013 to Workshop Numerical Methods for PDE Constrained Optimization with Uncertain Data, 2013.

[6] J. Rang, *Improved traditional Rosenbrock–Wanner methods for stiff ODEs and DAEs*, Informatikbericht 2013-05, TU Braunschweig, Braunschweig, 2013, URL: http://www.digibib.tu-bs.de/?docid=00055262.

[7] B. Rosić and J. Diekmann, *Non-intrusive methods for the uncertainty quantification of basic aircraft model (BACM)*, SFB 880 – Fundamentals of High-Lift for Future Commercial Aircraft, Biennial report (R. Radespiel and R. Semaan, eds.), TU Braunschweig, Campus Forschungsflughafen, 2013, pp. 204–216.

4.3 Vorträge

Noémi Friedman, *Stochastic analysis of the deployment pattern of an antiprismatic deployable space truss system*, GAMM 2013, 18-22 March 2013, Novi Sad, Serbia

Alexander Litvinenko, *Efficient Analysis of High Dimensional Data in Tensor Formats*, invited talk, KAUST, Saudi Arabia, April 2014

Alexander Litvinenko and Hermann G. Matthies, *Derivation and Low-rank Computation of the Bayesian Filter*, SIAM CSE, Boston, USA, February 2013

Alexander Litvinenko and W. Nowak, *Kriging, combining low-rank covariance approximations with FFT-techniques*, Project meeting at MIS MPG in Leipzig, April 2014

Alexander Litvinenko and H. G. Matthies, *Non-sampling functional approximation of linear and non-linear Bayesian Update*, Novi Sad, Serbia GAMM, 2013

Alexander Litvinenko and H. G. Matthies, *Non-sampling functional approximation of linear and non-linear Bayesian Update*, 29th GAMM-Seminar Leipzig on Numerical Methods for Uncertainty Quantification, January 21-23, 2013, MPI MIS Leipzig

Alexander Litvinenko, B. Khoromskij and H. G. Matthies, *Data sparse approximation of the Karhunen-Loève expansion*, Mini-workshop Numerical Upscaling for Media with Deterministic and Stochastic Heterogeneity, 10-6 Feb. 2013, Oberwolfach

Alexander Litvinenko and H. G. Matthies, *Sampling and Low-Rank Tensor Approximations*, Workshop Numerical Methods for PDE Constrained Optimization with Uncertain Data, 27 January-1 February 2013, Oberwolfach

Noémi Friedman, *Stochastic analysis of the deployment pattern of an antiprismatic deployable space truss system*, GAMM 2013, 18-22 March 2013, Novi Sad, Serbia

Hermann G. Matthies, invited talk *A stochastic setting for inverse identification problems*, 29th GAMM-Seminar on Numerical Methods for Uncertainty Quantification: Solving High-Dimensional Problems Arising from PDEs with Uncertain Parameters, Leipzig, 22 January 2013

Hermann G. Matthies, *Parametric problems, stochastics, and identification*, King Abdullah University of Science and Technology, Thuwal, Kingdom of Saudi Arabia, 6 March 2013

Hermann G. Matthies, Rainer Niekamp, Martin Krosche, Alireza Doostan, *Coupled Stochastic Field Problems*, Computational Methods in Marine Engineering V, Hamburg, 29 May 2013. nur abstract in online proceedings

Hermann G. Matthies, Semi-Plenary Lecture *Inverse and identification problems in continuum mechanics*, ECCOMAS and IACM Special Interest Conference, SEECCM III, Kos, Greece, 13 June 2013 keine proceedings gefunden

Hermann G. Matthies, *A model reduction approach for partitioned treatment of uncertainty in coupled problems*, V International Conference on Coupled Problems in Science and Engineering (COUPLED PROBLEMS 2013) - A Conference Celebrating the 60th Birthday of Eugenio Oñate, Ibiza, Spain, 18 June 2013 STIMMT DAS ODER HAT ALIREZA ODER WER ANDERS DEN VORTRAG GEHALTEN? nix in proceedings oder e-book

Rainer Niekamp, Martin Krosche, Alireza Doostan, Hermann G. Matthies, *Iterative methods for coupled stochastic field problems*, V International Conference on Coupled Problems in Science and Engineering (COUPLED PROBLEMS 2013) - A Conference Celebrating the 60th Birthday of Eugenio Oñate, Ibiza, Spain, 18 June 2013 nur abstract bei online proceedings

Hermann G. Matthies, *Stochastic Multiscale Coupling*, IUTAM Symposium on Multiscale Modeling and Uncertainty Quantification of Materials and Structures, Santorini, Greece, 8-11 September 2013 keine proceedings

Hermann G. Matthies, Mike Espig, Wolfgang Hackbusch, Alexander Litvinenko, Elmar Zander, Keynote Lecture *Analysis of Data in Tensor Formats*, 2nd International Workshop on Reduced Basis, POD and PGD model Reduction Techniques, Blois, France, 3-6 November 2013

Hermann G. Matthies, *Parametric Quantities, their Representations and Factorisations, and Inverse Identifications Methods* and *Parametric and stochastic Problems - an Overview of Computational Methods*, Workshop PDEs with Random Coefficients, WIAS Berlin, 13-15 November 2013

Joachim Rang, H. G. Matthies, *Stochastic Navier-Stokes equations are a coupled system*, Computational Methods in Marine Engineering V, Hamburg, 30 May 2013.

Joachim Rang, *Adaptive time step control with Rosenbrock-Wanner methods for the incompressible Navier-Stokes equations*, Vortrag beim GMS, Braunschweig, June 2013.

Joachim Rang, *Adaptive timestep control for the generalised-α method*, ADMOS, Lissabon, Portugal, June 2013.

Joachim Rang, *Coupling generalised-α methods: Analysis, adaptivity, and numerics*, Computational Methods for Coupled Problems in Science and Engineering V., Santa Eulalia, Ibiza, Spain, June 2013. proceedings http://congress.cimne.com/coupled2013/proceedings/full/p550.pdf

B. Rosić and O. Pajonk and A. Litvinenko and H. G. Matthies and A. Kučerová and J. Sŷkora. *Inverse Problems via linear Bayesian Identification.* GAMM, 84th Annual Meeting of the International Association of Applied Mathematics and Mechanics, Novi Sad, Serbia, March 2013

B. Rosić and H. G. Matthies and M. Živković and A. Ibrahimbegović. *Stochastic Description of Large Strain Elastoplasticity.* SEECCM III, 3rd South-East European Conference on Computational Mechanics, Kos Island, Greece, June 2013

B. Rosić. *Variational Formulations and Functional Approximation Algorithms in Stochastic Plasticity of Materials*, YIC2013, Second ECCOMAS Young Investigators Conference, Bordeaux, France, September 2013

B. Rosić, H. G. Matthies, M. Živković and A. Ibrahimbegović. *Uncertainty Quantification Methods for Elastoplastic Problems Described by Uncertain Paremeters.* COMPLAS XII, XII International Conference on Computational Plasticity. Fundamentals and Applications, Barcelona, Spain, September 2013

B. Rosić, Plenary lecture *Variational Formulations and Functional Approximation Algorithms in Stochastic Plasticity of Materials*,

GACM 2013, 5th GACM Colloquium on Computational Mechanics, Hamburg University of Technology (TUHH), Germany, October 2013

B. Rosić, Invited talk *Parameter Identification in a Probabilistic Setting*, Prirodno-matematički fakultet, Univerzitet u Kragujevcu, December 2013

4.4 Projekttreffen

Bojana Rosić, *Quantifizierung von Unsicherheiten*, SFB 880 Quartalstreffen im Projektbereich C, 12.04.2013

Noémi Friedman, *Quantifizierung von Unsicherheiten*, SFB 880 Quartalstreffen im Projektbereich C, 07.05.2013

Noémi Friedman, *Quantifizierung von Unsicherheiten*, SFB 880 Forschungsklausur, Braunlage, 23-24.09.2013

Joachim Rang, *Quantifizierung von Unsicherheiten*, SFB 880 internal review meeting, Braunschweig, 02.12.2013

A. Litvinenko, H.G. Matthias and E. Zander, *Quantifizierung von Unsicherheiten*, *Effective approaches and solution techniques for conditioning, robust design and control in the subsurface*, Stuttgart, 2013

Alexander Litvinenko and W. Nowak, *Kriging, combining low-rank covariance approximations with FFT-techniques*, Project meeting at MIS MPG in Leipzig, April 2014

4.5 Organisation von Minisymposia/Konferenzen

Hermann G. Matthies, Adnan Ibrahimbegović, Invited Session: Inelastic response of heterogeneous media. 12th International Conference on Computational Plasticity. Fundamentals and Applications (COMPLAS XII) 3-5 September 2013

Hermann G. Matthies, Radovan Slavković, Miroslav Živković, Bojana Rosić, Minisymposium: Problems with Heterogeneous Materials for the SEECCM III, Kos Island, Greece, 12-14 June 2013

Thorsten Grahs: Workshop NOFUN 2013 – Northern Germany OpenFoam User MeetiNg, Braunschweig, Haus d. Wissenschaften, 9.10.2013. With participants from DLR, FH Kiel, TU Berlin, TU Hamburg-Harburg, TU Braunschweig, Chalmers University Gothenburg, FutureShip, Engysy, u.a.

4.6 Teilnahme und Lehre an Workshops und Weiterbildung

Noémi Friedman, *Partial Differential Equations with Random Coefficients*, WIAS Berlin, 13.-15.11.2013

Noémi Friedman, *Flight Dynamics of Rigid and Flexible Aircraft*, DLR, short course, Braunschweig, 29.-30.08.2013

Hermann G. Matthies, *Non-linear Bayesian Updates*, Oberwolfach Workshop on Numerical Methods for PDE Constrained Optimization with Uncertain Data, Oberwolfach, 28-31 January 2013

Hermann G. Matthies, *Inverse Uncertainty Quantification*, Workshop on Numerical Methods for Uncertainty Quantification (NuMUQ, Hausdorff Center for Mathematics, University of Bonn, 13-17 May, 2013.

Hermann G. Matthies, *Analysis of Data in Tensor Formats*, 2nd International Workshop on Reduced Basis, POD and PGD model Reduction Techniques, Blois, France, 3-6 November 2013

Hermann G. Matthies, *Parametric Quantities, their Representations and Factorisations, and Inverse Identifications Methods* and *Parametric and stochastic Problems - an Overview of Computational Methods*, Workshop PDEs with Random Coefficients, WIAS Berlin, 13-15 November 2013

B. Rosić, 29th GAMM-Seminar Leipzig on Numerical Methods for UQ, Max-Planck-Institut Leipzig, Germany, January 2013.

4.7 Dissertationen

M. Krosche, A generic component-based software architecture for the simulation of probabilistic models, Ph.D. thesis 2012, Technische Universität Braunschweig, Druck 2013, http://www.digibib.tu-bs.de/?docid=00052792.

E. Zander, Tensor approximation methods for stochastic problems, PhD. thesis 2012, Technische Universität Braunschweig, Druck 2013, http://www.digibib.tu-bs.de/?docid=00053618

B. Rosić, Variational Formulations and Functional Approximation Algorithms in Stochastic Plasticity of Materials, Ph.D. thesis 2012, Technische Universität Braunschweig, Druck 2013, http://www.digibib.tu-bs.de/?docid=00052794

4.8 Abschluss- und Studienarbeiten

Krishna Kumar Sathyanarayana *MATLAB GUI: Implementierung - Statistik & Mining*, Studienarbeit. Betreuer: Joachim Rang

5 Sonstiges

In der Episode *123-Numerische Mathematik* spricht Prof. Hermann Matthies auf omega tau http://omegataupodcast.net/2013/04/123-numerische-mathematik/ über seine Arbeit am Institut für wissenschaftliches Rechnen der TU Braunschweig. Dabei geht es um Differentialgleichungen, Diskretisierungs- und Näherungsverfahren, aber auch um rechnergestützte Lösungsverfahren, Anwendungsbeispiele und aktuelle Forschungsthemen. April 2013

5.1 Gäste am Institut

Dr. Loïc Girardi, École Centrale Nantes, *Computational methods based on tensor approximations and applications to computational mechanics*, 14-18 January 2013

Dr.-Ing. Kheirollah Sepahvand, Institut für Mechanik an der Universität der Bundeswehr München, *Stochastic FEM model of biocomoposite structures with uncertain material properties*, 2-5 April 2013

Prof. Dr. habil. Hans-Jörg Starkloff, Westsächsische Hochschule Zwickau, *On polynomial chaos expansions and linear estimation for uncertainty quantification*, 5 April 2013

Dr. Venera Khoromskaia, Max-Planck Institute for Mathematics in the Sciences, *Basic formats and algorithms of the tensor numerical methods*, 24-25 April 2013

Dr. Boris Khoromskij, Max-Planck Institute for Mathematics in the Sciences, *Tensor methods for multi-parametric problems in uncertainty quantification*, 24-25 April 2013

Prof. Dr. Roland Herzog, TU Chemnitz, *An Introduction to Optimum Experimental Design*, 8 May 2013

Prof. Dr. Ekaterina Kostina, Philipps-Universität Marburg, *Efficient Methods for Parameter Estimation and Optimum Experimental Design for Dynamic Processes*, 3 June 2013

Dr. Michael Schick, Postdoc researcher Data Mining and Uncertainty Quantification, HITS gGmbH Heidelberg, *A non-intrusive and parallel multilevel spectral Galerkin solver for stochastic elliptic problems*, 24 June 2013

Assoc.-Prof. Dr. Dora Selesi, University of Novi Sad, *Chaos expansions methods for solving stochastic differential equations*, 22-30 June 2013

Prof. Dr. Roger Ohayon, Conservatoire National des Arts et Métiers (CNAM) Paris, *Modal Reduced Order Models for Fluid-Structure Interaction*, 7-11 May, 7-12 July, 20-27 November 2013

5.2 Einladungen an Mitglieder des Instituts

Hermann G. Matthies, invitation as visiting Professor to the King Abdullah University of Science and Technology, SRI Center for Uncertainty Quantification in Computational Science & Engineering, Thuwal, Kingdom of Saudi Arabia, 3-16 March 2013

5.3 Auszeichnungen

In December 2013 Professor Matthies was awarded Full Membership of the Braunschweigische Wissenschaftliche Gesellschaft, section Mathematics and Natural Sciences.

ScienceDirect judges the article *A multi-scale approach to model localized failure with softening* by Martin Hautefeuille, Jean-Baptiste Colliat, Adnan Ibrahimbegović, Hermann G. Matthies and Pierre Villon as **one of the Top 25 Hottest Articles** published in Computers & Structures in 2012. Listen to the AudioSlides Präsentation under http://www.youtube.com/watch?v=2BRv1VQW-eA.

Dr. Bojana Rosić was given the GACM Award for the best PhD Thesis on Computational Methods in Applied Sciences and Engineering at the 5th GACM Colloquium on Computational Mechanics (http://www.tuhh.de/gacm2013/homepage.html). The award was granted for the first time, and it is endowed with 1.000 Euros.
Dr. Rosić was also a finalist for the ECCOMAS Best PhD Thesis Award 2012 http://yic2013.sciencesconf.org/.

5.4 Board Memberships

Professor Matthies is Associate Editor for the *ASA- and SIAM Journal on Uncertainty Quantification* as well as a member of the Editorial Advisory Board for the recently launched journal *Advanced Modelling and Simulation in Engineering Sciences* (AMSES).
He is also a member of the Advisory Boards of the SRI - Center for Uncertainty Quantification in Computational Science Engineering at King Abdulla University of Science and Technology (KAUST), Saudi Arabia, and of the Editorial Board of Coupled Systems Mechanics (CSM).

5.5 Beteiligung am SFB 880 Grundlagen des Hochauftriebs künftiger Verkehrsflugzeuge

Wissenschaftliches Ziel dieses SFB ist es, die technologischen Grundlagen von neuartigen Hochauftriebskonzepten für lärmarme Verkehrsflugzeuge mit Kurzstart- und Kurzlandeeigenschaften zu schaffen. Dabei wirken zahlreiche Forschungsstellen (z.B. Aerodynamik, Akustik, Turbomaschinen u.v.m.) zusammen. Dies wird durch die Beteiligung der Forschungsinstitute der TU Braunschweig, das LU Hannover-Institut für Turbomaschinen und Fluid- Dynamik und durch eine wesentliche Beteiligung des Deutschen Zentrums für Luft- und Raumfahrt (DLR)in Braunschweig erreicht. Eine eingehende Analyse heutiger Verkehrsflugzeuge ergibt einen zukünftigen Bedarf für Hochauftriebssysteme, der nicht durch die derzeitig vorherrschende, evolutionäre Technologienentwicklung abgedeckt werden kann. Dieses gilt vor allem in den Bereichen der Lärmminderung und der verbesserten Skalierbarkeit der Leistungsparameter von Hochauftriebssystemen bei Start und Landung.

Das Teilprojekt „Quantifizierung der Unsicherheiten in Modellen der Hochauftriebsflugdynamik des Instituts für Wissenschaftl. Rechnens“ untersucht und charakterisiert die Robustheit des Fliegens in Hochauftriebskonfiguration und etwaiger Regelsysteme mit neuartigen, stochastischen Approximations-Verfahren. Bei der Modellierung derartiger Systeme treten meist Unsicherheiten auf, die durch nur ungenau bekannte Parameter, Messungen oder unbekannte Modelleinflüsse bedingt sind. Gegenwärtig wird die Quantifizierung von Unsicherheiten bei der Simulation des Flugverhaltens sowie die Berücksichtigung stochastischer dynamischer Vorgänge in der Atmosphäre in der Form von Monte-Carlo-Simulationen durchgeführt. Hier dagegen werden die Eingangsunsicherheiten und auch alle späteren Ergebnisse als Funktionen unabhängiger Zufallsvariablen modelliert. Um die Unsicherheiten bzgl. Rechenzeit und Speicherbedarf möglichst effizient quantifizieren zu können, wird eine Niedrig-Rang-Approximation mit dünnen Tensorproduk-

ten verwendet.

Ein Graduiertenkolleg ist in den SFB integriert.

Weitere Informationen zum SFB 880 finden Sie unter https://www.tu-braunschweig.de/sfb880

5.6 Beteiligung am Studiengang CSE

Professor Matthies ist stellvertretender Sprecher des internationalen Master-Studiengangs Computational Sciences in Engineering (CSE).

Der an der Technischen Universität Braunschweig zuerst angebotene und in Deutschland inzwischen kopierte Studiengang CSE wurde gegründet, um dem ständig wachsenden Bedarf der Industrie an qualifiertem Nachwuchs im Bereich Computersimulation gerecht zu werden. Er gibt Studierenden die Möglichkeit, eine spezifische Ingenieur- bzw. Naturwissenschaft zusammen mit dem Wissenschaftlichen Rechnen und der Informationsverarbeitung in einer internationalen und interdisziplinären Umgebung zu studieren.

Die internationale und interdisziplinäre Ausrichtung, die durch die englische Sprache, einen einsemestrigen Auslandsaufenthalt an einer Partneruniversität für deutsche Studierende sowie die Kooperation unterschiedlicher Studiengänge gegeben ist, erweitert die beruflichen Möglichkeiten der Absolventen entscheidend. Die Studienschwerpunkte liegen in den Bereichen Mechanik, Angewandte Mathematik und Angewandte Informatik.

Weitere Informationen zum Studiengang CSE findet man unter http://www.tu-braunschweig.de/cse.